Geotechnique

Foundation punch-through in clay with sand: analytical modelling

--Manuscript Draft--

Manuscript Number:	16-P-101R3
Full Title:	Foundation punch-through in clay with sand: analytical modelling
Article Type:	General Paper
Corresponding Author:	Shah Neyamat Ullah, PhD National University of Singapore Singapore, SINGAPORE
Corresponding Author's Institution:	National University of Singapore
Order of Authors:	Shah Neyamat Ullah, PhD
	Samuel Stanier, PhD
	Yuxia Hu
	David White
Corresponding Author's Secondary Institution:	
Order of Authors Secondary Information:	
Manuscript Region of Origin:	AUSTRALIA
Abstract:	Severe punch-through of jack-up rig foundations can occur due to the presence of a stronger sand layer in a bed of relatively soft clay. Analytical estimation of the bearing capacity and leg load-penetration response on such multi-layer stratigraphies is challenging. Accurate mechanism-based models need to be established in each of the layers involved and the effects of the mechanisms in each of the layers on the response in the other layers must be captured. Based on the recently-developed failure stress-dependent punch-through models for sand-clay stratigraphies, an extended model is proposed for clay-sand-clay stratigraphies. Half-spudcan PIV (Particle Image Velocimetry) centrifuge tests and full-spudcan centrifuge tests are used in developing and validating the extended model. The centrifuge test results were discussed in the companion paper (Ullah et al., 2016) and this paper focuses on the analytical developments and prediction assessment. Both spudcan peak resistance (qpeak) and spudcan punch-through depth (dpunch) can be estimated using the model. The predictions by the extended model and by the current industry guidelines (ISO, 2012) are compared against the centrifuge test data. The extended model proposed in this paper outperforms the approaches suggested in the guidelines. An advantage of the proposed approach is that it can be used for either sand-clay or clay-sand-clay scenarios and exhibits excellent performance compared to the model testing dataset considered in this work for both cases. The resulting penetration resistance model is a useful design tool for routine punch-through risk assessment.
Suggested Reviewers:	
Opposed Reviewers:	
Additional Information:	
Question	**Response**
Please enter the total number of words in the main text only. The main text of the paper should be as concise as possible. The word count of General Papers should not exceed 5000 words and for Technical Notes should not	6260

exceed 2000 words. The word count of a submission excludes the abstract, list of notation, acknowledgements, references, tables and figure captions. Discussions, Book Reviews, and Obituaries should be less than 1000 words. Whilst Geotechnique reserves the right to publish papers of any length Authors should be aware that any submission for a General Paper that is significantly over the word limit will be subjected to pre-assessment and may be returned to the Authors for editing prior to being sent for review. The word limit for Technical Notes will be strictly adhered to, and if over 2000 words, the submission will be considered as a General Paper.	
Have you included a full notation list including definitions (and SI units of measurement where appropriate) for any mathematical terms and equations included in your paper?	Yes
Have you included a completed copyright transfer form? This is required for all publications and can be found here.	Yes
Have you uploaded each of your figures separately and in high-resolution .tiff (ideal for photographs) or .eps files (best for line drawings)? This is required for all figures before your paper can be accepted. Our figure requirements can be found here.	Yes
Have you uploaded your tables in an editable Microsoft Word (.doc) format?	Yes
Have you included a separate list of all your figure and table captions?	Yes
Are your figures clear when printed in black and white? (For example, are plot lines distinguishable; are tints sequentially graded?) As this journal is printed in black and white, any figures that are unclear may be removed.	Yes
Are your references in Harvard style? Our reference guidelines can be found here.	Yes
To ensure your paper is indexed correctly – and therefore as discoverable as possible – in our ICE Virtual Library, please choose up to 6 keywords from our Keywords List. This can be found here. We are unable to accept keywords that do not appear on this list.	Bearing capacity, Centrifuge modelling, Footings/foundations, Model tests, Offshore engineering, Soil/structure interaction
Manuscript Classifications:	Bearing capacity; COASTAL, MARINE AND OFFSHORE GEOTECHNICS; FOUNDATIONS AND SOIL-STRUCTURE INTERACTION; Offshore foundations; Spudcan foundations
Author Comments:	This is the second part of the companion paper. This includes supplementary data.

Date of Writing-12/04/2016

Title of Submission- Foundation punch-through in clay with sand: analytical modelling

Authors:

i) Shah Neyamat Ullah (corresponding author)

PhD

Research Fellow, Department of Civil and Environmental Engineering

National University of Singapore

(Telephone +65 9814 2663, Email: shahneyamat.ullah@nus.edu.sg)

ii) Samuel Stanier

PhD

Research Fellow, Centre for Offshore Foundation Systems

University of Western Australia, Crawley, WA 6009, Australia.

Email: sam.stanier@uwa.edu.au

iii) Yuxia Hu

PhD

Professor, School of Civil Environmental and Mining Engineering

University of Western Australia, Crawley, WA 6009, Australia.

Email: yuxia.hu@uwa.edu.au

iv) David White

PhD

Professor, Centre for Offshore Foundation Systems

University of Western Australia, Crawley, WA 6009, Australia.

Email: david.white@uwa.edu.au

Words: Main text (Introduction to Conclusion) = 6260; Abstract =239;

Figures: 14

Tables: 1

FOUNDATION PUNCH-THROUGH IN CLAY WITH SAND: ANALYTICAL MODELLING

Shah Neyamat Ullah, Samuel Stanier, Yuxia Hu and David White

ABSTRACT

Severe punch-through of jack-up rig foundations can occur due to the presence of a stronger sand layer in a bed of relatively soft clay. Analytical estimation of the bearing capacity and leg load-penetration response on such multi-layer stratigraphies is challenging. Accurate mechanism-based models need to be established in each of the layers involved and the effects of the mechanisms in each of the layers on the response in the other layers must be captured. Based on the recently-developed failure stress-dependent punch-through models for sand-clay stratigraphies, an extended model is proposed for clay-sand-clay stratigraphies. Half-spudcan PIV (Particle Image Velocimetry) centrifuge tests and full-spudcan centrifuge tests are used in developing and validating the extended model. The centrifuge test results were discussed in the companion paper (Ullah et al., 2016) and this paper focuses on the analytical developments and prediction assessment.

Both spudcan peak resistance (q_{peak}) and spudcan punch-through depth (d_{punch}) can be estimated using the model. The predictions by the extended model and by the current industry guidelines (ISO, 2012) are compared against the centrifuge test data. The extended model proposed in this paper outperforms the approaches suggested in the guidelines. An advantage of the proposed approach is that it can be used for either sand-clay or clay-sand-clay scenarios and exhibits excellent performance compared to the model testing dataset considered in this work for both cases. The resulting penetration resistance model is a useful design tool for routine punch-through risk assessment.

1. INTRODUCTION

Oil and gas recovery in shallow to medium water depths (up to ~150 m) is commonly carried out from self-elevating jack-up rigs. Jack-up rigs are supported by quasi-circular or sometimes polygonal shaped foundations, commonly referred to as spudcans. Punch-through of spudcan

foundations remains the most common cause of failure of jack-up rig deployment (Osborne and Paisley, 2002). Installation of spudcan foundations in clay with interbedded sand (clay-sand-clay profile) can lead to catastrophic punch-through failure, where the foundation leg penetrates uncontrollably for several metres before stabilising in the underlying clay (Figure 1). Such stratigraphies are common to many offshore sites such as Gulf of Suez, Southeast Asia, Gulf of Mexico and offshore South America (Baglioni et al., 1982; Dutt and Ingram, 1984; Teh et al., 2009) and have led to fatalities to operational personnel (Dier et al., 2004).

Accurate models for predicting the peak resistance during punch-through failure on sand-clay stratigraphies have been developed (Figure 2). Lee et al. (2013a) conducted centrifuge experiments and small-strain finite element (FE) numerical simulations for dense sand (relative density, I_D = 92%) overlying clay resulting in the development of a simplified conceptual model to predict the peak punch through capacity q_{peak} (see Lee et al., 2013b and Figure 2a). Hu et al. (2014a) modified the model further to account for the depth of embedment during mobilisation of the peak resistance (Figure 2b) and validated the model for medium dense sand on clay (I_D = 44%). Simple methods for predicting the penetration resistance profile for sand-clay stratigraphies have also been proposed (Hu et al. 2014b).

However, no validated analytical model exists for stratigraphies involving more than two layers. The current industry guidelines (SNAME, 2008; ISO, 2012) recommend soil models originally developed for two layers (either the punch-through model for strong over soft soil such as sand-clay, or the squeezing model for soft over strong soil such as clay-sand). However, no specific guidelines are provided for the application of these methods for either clay-sand-clay or sand-clay-sand scenarios. Furthermore, these basic models have already been shown to generate poor predictions for sand-clay stratigraphies (Hu et al. 2015a), primarily because of their inability to account for the stress-level dependent behaviour of sand (i.e. the friction angle changing with ambient stress level). In addition, image analysis of multi-layered punch-through centrifuge experiments (see Teh et al. 2008; Hossain, 2014; Hu et al. 2015b; Ullah et al. 2016) indicate that some of the overlying soil becomes entrapped beneath the spudcan foundation during penetration, leading in some instances to increased penetration resistance but a less severe punch-through event. The simple models recommended by SNAME and ISO do not account for these entrapped layers of soil, causing the models to significantly under-

predict the penetration resistance during punch-through, and often overpredict the risk associated with uncontrolled leg penetration (Ullah et al. 2015).

This paper develops an analytical method to predict the penetration resistance profile for jack-up foundations on clay-sand-clay stratigraphies, which can be generalised to higher numbers of layers. The method incorporates simple models for the penetration resistance in the top clay layer, the peak resistance in the sand layer and the penetration resistance in the underlying clay layer. The models in different layers are developed based on the failure mechanisms observed in the experiments in which image analysis was used to determine the soil deformation patterns (White et al. 2003, Stanier et al. 2016) (see Figure 3). The peak resistance model incorporates a modified version of Bolton's (1986) equations to capture the stress-level dependent response of the sand layer during punch-through. Moreover, the peak resistance model extends the approaches reported by Lee et al. (2013b) and Hu et al. (2014a), where the top clay layer height is zero. In this way, the clay-sand-clay model developed here can be easily simplified to the two-layer model without the top clay layer (i.e. sand-clay), assuming that for both the soil stratigraphies the sand and clay shearing is in a drained and undrained manner respectively. All models are formulated in terms of soil parameters that have clear physical meanings and can be determined from standard offshore investigations. The method is validated against a series of centrifuge model tests that covers a range of clay-sand-clay layer geometries and soil properties.

2. EXTENDED STRESS DEPENDENT MODEL FOR q_{peak}

The primary calculation when assessing punch-through potential for stratigraphies involving thin sand layers is the peak resistance mobilised in the sand layer (q_{peak}), as loading the jack-up foundation to a level higher than this pressure usually initiates the punch-through failure if the underlying layers are comparably weak. When assessing the potential severity of punch-through failure, the bearing capacity in the over, and underlying clay layers must also be predicted to form a complete penetration response, which will be discussed later in this paper. Based on the complete penetration profile of the spudcan, the punch-through depth can be determined, when an equilibrium is re-established in the underlying weaker layer and punch-through failure ceases.

The q_{peak} model for clay-sand-clay is an extension to the sand-clay model of Hu et al. (2014a). The geometry of the mechanism is based on observations of soil deformation described in the companion paper (Ullah et al., 2016) and is illustrated in Figure 4. In essence, a frustum of sand underneath the spudcan punches through into the underlying clay layer with the spudcan. The sand frustum has a spreading angle to the vertical approximately equal to the dilation angle (ψ) of the sand. The mechanism of three layers (clay-sand-clay) is similar to that of two layers (sand-clay) described by Hu et al. (2014a) with the following additions:

1. A layer of clay of height H_c is entrapped between the spudcan and the sand frustum, based on the soil deformation observations of Ullah et al. (2016);
2. As a result, the depth at which the peak resistance is mobilised, d_{peak} is less than that for the two-layer sand-clay case; and
3. Partial backflow of the top layer of clay above the spudcan occurs prior to the mobilisation of q_{peak}.

The following sections describe how these additions are considered in the three-layer (clay-sand-clay) model based on the two-layer (sand-clay) model of Hu et al. (2014a).

3. MATHEMATICAL FORMULATION FOR PEAK RESISTANCE q_{peak}

Based on vertical equilibrium of a thin horizontal disk element (Figure 4b) the following differential equation is formed (following Lee et al., 2013b and Hu et al., 2014a):

$$\frac{d\sigma_z^{'}}{dz}+\frac{2\left[\tan\psi+D_F\left(\tan\varphi^{*}-\tan\psi\right)\right]\sigma_z^{'}}{R+z\tan\psi}-\gamma_s^{'}=0 \qquad (1)$$

D_F is the ratio between the effective normal stresses acting on the sides of the sand frustum and the mean vertical stress within the frustum. Mathematically:

$$D_F=\frac{\sigma_n^{'}}{\sigma_z^{'}} \qquad (2)$$

φ^* is a reduced friction angle due to non-associated flow of sand, obtained from the expression proposed by Drescher and Detournay (1993) as:

$$\tan\varphi^{*}=\frac{\sin\varphi'\cos\psi}{1-\sin\varphi'\sin\psi} \qquad (3)$$

Following Lee et al. (2013b) and Hu et al. (2014a), Equation 1 can be simplified by introducing a simplification parameter E:

$$\frac{d\sigma_z^{'}}{dz}+\frac{E\tan\psi\sigma_z^{'}}{R+z\tan\psi}-\gamma_s^{'}=0 \quad (4)$$

where:

$$E=2\left[1+D_F\left(\frac{\tan\varphi^*}{\tan\psi}-1\right)\right] \quad (5)$$

The stress ratio of D_F was related to the normalised height of the sand layer (H_s/D) based on the empirical study by Hu et al. (2015c). This empirical power law is also adopted here:

$$D_F(\text{spudcan})=0.642\left(\frac{H_s}{D}\right)^{-0.576};0.16\le\frac{H_s}{D}\le1.0 \quad (6)$$

$$D_F(\text{flat})=0.623\left(\frac{H_s}{D}\right)^{-0.174};0.21<\frac{H_s}{D}<1.12 \quad (7)$$

Equations 6 & 7 provide a slightly higher value of D_F for a spudcan. The higher D_F value for a spudcan reflects the probable generation of increased lateral stresses during q_{peak} mobilisation due to the conical underside, as illustrated in Lee et al. (2013b), which was also demonstrated by the higher accumulated radial strains underneath the spudcan by Hu et al. (2015b).

Equation 1 can be directly integrated by assuming E is constant to give the following form:

$$\left(R+z\tan\psi\right)^E\sigma_z^{'}=\frac{\gamma_s^{'}\left(R+z\tan\psi\right)^{E+1}}{\tan\psi\left(E+1\right)}+C \quad (8)$$

where C is the integration constant and can be evaluated from the first boundary condition as: at $z = H_{eff}$, the vertical stress σ'_z equates to the bearing capacity of the underlying clay layer q_{clay} (Figure 4). The bearing capacity of the underlying clay q_{clay} is defined after Lee et al. (2013b) as:

$$q_{clay}=N_{co}s_{ubi}+q_o+H_{ct}\gamma_{ct}^{'}+H_{eff}\gamma_s^{'}+0.12H_s\gamma_s^{'}+\text{sign}(H_{ct})\frac{4V_f}{\pi D^2}\gamma_{ct}^{'} \quad (9)$$

where s_{ubi} is the bottom intercept strength, q_o is the surcharge, γ'_{ct} and γ'_s are the top clay and sand effective unit weights, respectively. The last term of Equation 9 is due to surface heave

where V_f is the volume of the embedded foundation. Soil deformation observations of Teh et al. (2008) showed that the sand around the periphery of the spudcan did not heave, so the last term is taken as zero when H_{ct} is zero (i.e. sign(0) = 0). When $H_{ct} = 0$ Equation 9 reduces to the clay bearing capacity for sand-clay stratigraphies, and when H_s is zero (i.e. H_{eff} is also zero) the bearing capacity of a single layer of clay is recovered.

The bearing capacity factor N_{co} is obtained from expressions provided by Houlsby and Martin (2003) for a rough circular foundation as:

$$N_{co} = 6.34 + 0.56\kappa \qquad 10$$

where κ is the normalised bottom clay strength gradient and is taken as:

$$\kappa = \frac{\rho_{cb}\left\{D + 2\left(H_{eff} + H_c\right)\tan\psi\right\}}{s_{ubi}} \qquad 11$$

where, ρ_{cb} is the bottom clay strength gradient and ψ is the inclination from vertical of the failure surface in the sand layer (see Figure 4), which is taken as equal to the sand dilatancy angle. κ lies within $0 \leq \kappa \leq 5$. Equation 10 is the best fit of the tabulated data provided by Houlsby and Martin (2003) with a discrepancy always less than 5%.

Therefore, the integration constant C can be evaluated as:

$$C = \left(R + H_{eff}\tan\psi\right)^{E}\left[\begin{array}{l}\left(N_{co}\,s_{ubi} + q_o + H_{ct}\gamma'_{ct} + H_{eff}\gamma'_s + 0.12H_s\gamma'_s + \text{sign}(H_{ct})\dfrac{4V_f}{\pi D^2}\gamma'_{ct}\right) \\ -\dfrac{\gamma'_s\left(R + H_{eff}\tan\psi\right)}{\tan\psi\left(E+1\right)}\end{array}\right] \qquad 12$$

By substituting C into Equation 8, taking H_{eff} as $0.88H_s$ (after Ullah et al., 2016), replacing foundation radius R by $\frac{D}{2}$ and applying the second boundary condition as: at $z = -H_c$, the mean vertical stress (σ'_z) equates to the peak bearing capacity q_{peak}, then the peak resistance q_{peak}, where $\varphi' > \varphi_{cv}$, can be expressed as:

$$q_{peak} = \left(N_{co}\, s_{ubi} + q_o + 0.12 H_s \gamma_s^{'} + H_{ct} \gamma_{ct}^{'} + \text{sign}(H_{ct}) \frac{4V_f}{\pi D^2} \gamma_{ct}^{'} \right) \left(1 + \frac{1.76 H_s}{D} \tan\psi \right)^E \quad 13$$

$$+ \frac{\gamma_s^{'} D}{2 \tan\psi \left(E + 1 \right)} \left[1 - \left(1 - \frac{1.76 H_s}{D} E \tan\psi \right) \left(1 + \frac{1.76 H_s}{D} \tan\psi \right)^E \right] +$$

$$\left[\tau_c \cos\psi - f_1 H_{ct} \gamma_{ct}^{'} - f_2 H_{ct} \gamma_{ct}^{'} \right] \quad \le q_{sand}; \qquad \text{for } \varphi' > \varphi_{cv}$$

where E is as defined in Equation 5, τ_c is the shear stress generated by shearing along the periphery of the entrapped clay layer and f_1 and f_2 are fractions of the top clay layer height. The factors f_1 and f_2 represent the fractions of the top clay layer height that become entrapped beneath the foundation and backflow on to the top of the foundation at mobilisation of the peak resistance, respectively.

The inequality at the end of Equation 13 is to limit the bearing capacity to that of a circular foundation resting on a deep layer of sand (q_{sand}) with surcharge $q_{o(s)}$:

$$q_{sand} = s_\gamma N_\gamma \frac{\gamma'_s D}{2} + s_q N_q q_{o(s)} \quad 14$$

$$q_{o(s)} = q_o + H_{ct} \gamma'_{ct} + \text{sign}(H_{ct}) \frac{4V_f}{\pi D^2} \gamma'_{ct} \quad 15$$

where s_γ, s_q and N_γ, N_q in q_{sand} are the shape and bearing capacity factors, respectively, which are taken from Hansen (1970).

The soil deformation analyses of Ullah et al. (2016) indicated that the average entrapped clay layer height H_c was 7% of the top clay layer height; hence f_1 is recommended as 0.07. Similarly, on average, half of the top clay layer height flowed back onto the top of the foundations; hence f_2 is recommended as 0.5.

The shear stresses on the periphery of the entrapped clay beneath the foundation (τ_c) are limited by the shear strength of the clay within the plug. The visualisation experiments indicated the entrapped clay consisted of a mix of soft material from near the mud line and stronger material from the sand surface (i.e. the upper clay-sand interface). For simplicity, the strength of the clay within the entrapped clay plug has been taken as the average strength of the top clay layer, thus:

$$\tau_c \cos\psi = \frac{0.28H_{ct}\left(s_{um} + \frac{\rho_{ct}H_{ct}}{2}\right)\left(D + 0.07H_{ct}\tan\psi\right)}{D^2} \quad (16)$$

Substituting τ_c of Equation 16, $f_1 = 0.07$ and $f_2 = 0.5$ into Equation 13 yields:

$$q_{peak} = \left(N_{co}\, s_{ubi} + q_o + 0.12H_s\gamma_s' + H_{ct}\gamma_{ct}' + \text{sign}(H_{ct})\frac{4V_f}{\pi D^2}\gamma_{ct}'\right)\left(1 + \frac{1.76H_s}{D}\tan\psi\right)^E + \frac{\gamma_s' D}{2\tan\psi\left(E+1\right)}\left[1 - \left(1 - \frac{1.76H_s}{D}E\tan\psi\right)\left(1 + \frac{1.76H_s}{D}\tan\psi\right)^E\right] + \left[\frac{0.28H_{ct}\left(s_{um} + \frac{\rho_{ct}H_{ct}}{2}\right)\left(D + 0.07H_{ct}\tan\psi\right)}{D^2} - 0.07H_{ct}\gamma_{ct}' - 0.5H_{ct}\gamma_{ct}'\right] \leq q_{sand}\,; \text{for } \varphi' > \varphi_{cv} \quad (17)$$

The effective height of the sand layer (i.e. the height of the sand layer when mobilising q_{peak}, measured as an average across the diameter of the foundation) was on average 88% of the original height of the sand layer in this study. This measurement is in agreement with the previous investigations from two-layer sand-clay tests by Teh et al. (2008) and Hu et al. (2015a). Referring to the diagram in Figure 4, the spudcan penetration depth at q_{peak} is:

$$d_{peak} = 0.93H_{ct} + 0.12H_s \quad (18)$$

This relationship implies that greater entrapped clay height (H_c) leads to reduced d_{peak} because the entrapped clay effectively increases the foundation thickness causing earlier peak resistance mobilisation. If the top clay height H_{ct} is set to zero, H_c becomes zero and d_{peak} simplifies to that suggested by Teh et al. (2010) for sand-clay stratigraphies.

3.1 Peak resistance when $\varphi' = \varphi_{cv}$ (i.e. loose sand)

For the case where $\varphi' = \varphi_{cv}$, then $\psi = 0$ and q_{peak} can be calculated as:

$$q_{peak} = \left(N_{co}\, s_{ubi} + q_o + 0.12 H_s \gamma_s^{'} + H_{ct} \gamma_{ct}^{'} + \text{sign}(H_{ct}) \frac{4V_f}{\pi D^2} \gamma_{ct}^{'} \right) e^{E_o} \quad 19$$

$$+0.88 H_s \gamma_s^{'} \left[e^{E_o} \left(1 - \frac{1}{E_o} \right) + \frac{1}{E_o} \right] + \left[\frac{0.28 H_{ct} \left(s_{um} + \frac{\rho_{ct} H_{ct}}{2} \right)}{D} - 0.07 H_{ct} \gamma_{ct}^{'} - 0.5 H_{ct} \gamma_{ct}^{'} \right] \le q_{sand} \text{ ; for } \varphi' = \varphi_{cv}$$

where E_o is taken as,

$$E_o = 3.52 D_F \sin \varphi_{cv} \frac{H_s}{D} \quad 20$$

Equations 17 and 19 are mathematically equivalent when the dilation angle ψ is close to zero.

3.2 Peak resistance when $H_{ct} = 0$

Substituting $H_{ct} = 0$ into Equation 17, the equation for q_{peak} when $\varphi' > \varphi_{cv}$ for two layer sand overlying clay reduces to:

$$q_{peak} = \left(N_{co}\, s_{ubi} + q_o + 0.12 H_s \gamma_s^{'} \right) \left(1 + \frac{1.76 H_s}{D} \tan \psi \right)^E \quad 21$$

$$+ \frac{\gamma_s^{'} D}{2 \tan \psi (E+1)} \left[1 - \left(1 - \frac{1.76 H_s}{D} E \tan \psi \right) \left(1 + \frac{1.76 H_s}{D} \tan \psi \right)^E \right] \le q_{sand}$$

Equation 21 is identical to that proposed by Hu et al. (2014a), demonstrating that the three layer model extension developed in this paper is universally applicable to both sand-clay and clay-sand-clay stratigraphies.

Similarly, setting $H_{ct} = 0$ in Equation 19, the equation for q_{peak} where $\varphi' = \varphi_{cv}$ reduces to:

$$q_{peak} = \left(N_{co}\, s_{ubi} + q_o + 0.12 H_s \gamma_s^{'} \right) e^{E_o} + 0.88 H_s \gamma_s^{'} \left[e^{E_o} \left(1 - \frac{1}{E_o} \right) + \frac{1}{E_o} \right] \le q_{sand} \quad 22$$

where E_o is given by Equation 20. This form is also identical to that given by Hu et al. (2014a) for loose sand-clay stratigraphies where $\varphi' = \varphi_{cv}$.

4. IMPLEMENTATION OF THE q_{peak} MODEL FOR CLAY-SAND-CLAY

4.1 Iterative procedure for estimating the operative friction and dilation angles

The angles of friction and dilation: φ' and ψ of sand can be related to each other using Bolton's equations (Bolton, 1986). Based on the work by Lee et al. (2013b), for the foundation peak resistance (q_{peak}), modified Bolton's equations are used taking the parameter m, which scales the relative dilatancy to determine the peak friction angle, as 2.65 so that:

$$I_R = I_D(Q - \ln q_{peak}) - 1, \qquad 0 \le I_R \le 4 \tag{23}$$

$$\varphi' = \varphi_{cv} + 2.65 I_R \tag{24}$$

$$0.8\psi = \varphi' - \varphi_{cv}, \quad \psi \ge 0 \tag{25}$$

Assuming that the in-situ relative density I_D, the natural logarithm of the grain crushing strength Q (in kPa; Q≈10 for siliceous sand) and critical state friction angle φ_{cv} are known, an iterative solution procedure can be used to obtain q_{peak}, since I_R is a function of q_{peak}. The iterative procedure can be performed by initially assuming an arbitrary value of ψ, allowing φ' to be estimated using Equation 25. Equations 17, 23, 24, and 25 are then applied iteratively in sequence to generate predictions for q_{peak}. After each iteration, the q_{peak} prediction is fed back into the system of equations to generate new values for φ' and ψ. The process is repeated, until the input and output values of q_{peak} converge. In this manner, the dependency of the operative friction and dilation angle on the failure stresses are incorporated into the analytical model. The iteration can easily be incorporated into the type of spreadsheet programmes commonly used to generate profiles of jack-up leg penetration resistance.

4.2 Summary of parameters required for q_{peak} prediction

All the parameters required to estimate q_{peak} have clear physical meaning and can be obtained from routine site investigation or laboratory tests. A description of the required parameters is given in Table 1.

5. PERFORMANCE OF THE EXTENDED q_{peak} MODEL

The performance of the extended clay-sand-clay model for the peak resistance during punch-through is verified by 27 new centrifuge model test results (Ullah et al., 2016). These tests were

conducted on samples consisting of medium dense to dense sand (I_D = 51-74%) interbedded in clay with strength increasing with depth. Details of the centrifuge modelling apparatus and techniques are reported in the companion paper (Ullah et al., 2016). In addition, three model test responses in denser sand (I_D = 89%) reported previously by Hossain (2014) have also been included in verification.

Moreover, the q_{peak} prediction using the extended model is compared to the guidelines documented in ISO (2012), where the projected area (also known as load-spread) and the punching-shear methods are recommended (see Figure 5). Some ambiguity exists in the ISO guidelines in whether the weight of the sand frustum should be considered when calculating the surcharge term in the formulae for both methods (Hu et al., 2015a). Thus in the comparisons showed in Figure 6, include cases which include (solid markers) and exclude (hollow markers) the weight of the sand frustum (W_{SF}) in the surcharge term. The effect of the additional top clay height (H_{ct}) was considered by replacing the surcharge term q_o with the product of the clay layer height and its effective unit weight of $H_{ct}\gamma'_{ct}$.

The punch-through method of Teh (2007) is recommended as an alternative calculation method for sand-clay stratigraphies in ISO (2012) (see also Figure 5c). To account for the additional top clay layer (H_{ct}) the peak bearing capacity (q_{peak}) equation of Teh (2007) has been extended (for which a full derivation is documented in the Appendix) as:

$$q_{peak}\frac{\pi D^2}{4} = \pi\left(N_{co}s_{ubi} + H_s\gamma'_s + H_{ct}\gamma'_{ct}\right)\left[R^2 - \frac{0.5}{R-r}\left(\frac{2}{3}R^3 + \frac{1}{3}r^3 - R^2 r\right)\right] \quad (26)$$

$$+\frac{\pi\gamma'_s K_p \sin\left(\varphi_2 - \psi_t\right)}{\cos\varphi_2 \cos\psi}\left[\begin{array}{l}\left(d_{peak} + \frac{1}{2}H_{eff}\right)DH_{eff} + d_{peak}\tan\psi_t H_{eff}^{\ 2} + \frac{2}{3}\tan\psi_t H_{eff}^{\ 3} \\ + \frac{H_{ct}\gamma'_{ct}}{\gamma'_s}H_{eff}\left(\tan\psi_t H_{eff} + D\right)\end{array}\right]$$

$$-\frac{1}{3}\pi H_{eff}\left[\left(\frac{D}{2}\right)^2 + R\frac{D}{2} + R^2\right]\gamma_s'$$

where the first term represents the clay bearing capacity, the second term represents the sand shear resistance and the third term is the effective sand frustum weight. R, r and ψ_t are

geometric parameters and φ_2 is the mean of operative and constant volume friction angle i.e. $(\varphi'+\varphi_{cv})/2$, while d_{peak} is taken as $0.12H_s$.

The effect of H_{ct} is to augment the peak capacity by increasing the sand shearing resistance and the bottom clay bearing capacity. If the top clay layer thickness, H_{ct}, is set to zero, the above equation reduces to that of Teh (2007) for sand-clay stratigraphies.

With the available centrifuge test results, Figure 6 depicts the performances of the industry guidelines (Figures 6a~6d) (projected-area and punching-shear models), the Teh (2007) model extended with surcharge (Figure 6e) and the three layer clay-sand-clay model developed in this paper (Figure 6f). The projected area and punching shear approaches of ISO (2012) are highly conservative, significantly under-predicting q_{peak} (Figures 6a~6d). Excluding the weight of the sand frustum (hollow markers in Figure 6) makes the prediction of q_{peak} closer to the test data. The Teh's (2007) model with extension to three layers performs better than both the projected-area and punching-shear approaches (Figure 6e). The three-layer clay-sand-clay model out-performs all of the other models, with most tests predicted within 20% variation bounds and the ratio of measured to predicted values of q_{peak} very close to unity at 1.05 (Figure 6f). In addition, the standard deviation (SD) and coefficient of variation (COV) of the predictions by the three-layer model are the lowest among all the models, indicating the reliability of the predictions.

6. PREDICTION METHOD FOR PENETRATION RESISTANCE PROFILE

To ascertain the potential depth of punch-through failure (d_{punch}) in layered soils, a complete penetration resistance profile in all soil layers needs to be established. Thus, it is necessary to predict the resistance in the over, and underlying clay layers, especially the spudcan resistance in the underlying clay layer, in order to determine where the peak resistance can be recaptured.

6.1 Penetration resistance estimation in the top clay layer ($q_{clay\text{-}ct}$)

The following equation is recommended to predict the resistance in the top clay layer:

$$q_{clay-ct} = N_c s_u + q_o + \frac{4V_f}{\pi D^2}\gamma'_{ct} \quad (27)$$

The first term is the soil resistance, q_o is the surcharge at the base of the foundation and the last term represents the buoyancy of the foundation in which V_f is the volume of the foundation where γ'_{ct} is the top clay effective unit weight. The bearing capacity factor N_c in single clay layer by Houlsby and Martin (2003) is adopted in Equation 27.

By comparing the centrifuge test data and the N_c factors by Houlsby and Martin (2003) in three-layer clay-sand-clay soils, Ullah et al. (2016) observed that at a certain depth in the upper clay layer the spudcan penetration resistance from the centrifuge test deviates from that predicted by Houlsby and Martin's (2003) solution (as point (q_d, d_d) in Figure 7a). This depth is defined as the depth of deviation d_d. Beyond the deviation depth d_d, a transition takes place until the peak resistance is reached. During the transition, the spudcan resistance changes from the top clay mechanism (Figure 7b) to the peak resistance mechanism (Figure 7c). Since the mobilisation of the sand layer generates a large increment in spudcan resistance over a relatively short penetration depth, the spudcan bearing capacity increases sharply and almost linearly (Figure 1b).

The industry guidelines provided by ISO (2012) suggest that squeezing (characterised by significant lateral displacement of soils) will occur in a soft layer when a foundation is in close proximity to an underlying stiff layer. In the guidelines the onset of squeezing is defined by the following criterion:

$$D \geq 3.45\left(H_{ct} - d\right)\left(1+1.025\frac{d}{D}\right) \text{ for } \frac{d}{D} \leq 2.5 \qquad 28$$

When the criterion is satisfied, squeezing is assumed to occur and the penetration resistance is estimated after Meyerhof and Chaplin (1953) rather than using conventional bearing capacity theory.

To examine the squeezing mechanism, Figure 8a presents the comparisons between centrifuge test results for clay-sand-clay soils by Hossain (2014) (the arrow indicates the tests with increasing H_s/D) and the squeezing solution by ISO (2012), together with the solution for single clay layer (Houlsby and Martin, 2003).

In the centrifuge tests the geometry and properties of the top clay layer were identical (H_{ct}/D = 0.62, s_{um} = 0.5 kPa and ρ_{ct} = 0.75 kPa/m), and the sand layer had the same relative density of

I_D = 89% but varying sand layer thickness ratio of H_s/D = 0.25 to 0.67. It is clear that the squeezing solution from ISO (2012) is independent from the sand layer stiffness (i.e. sand I_D and H_s/D) and the centrifuge test results show otherwise. At the same time, the depth of deviation d_d is dependent on the sand layer stiffness as well. Similar results are obtained for spudcan test in Figure 8b (test SPa16 reported by Ullah et al., 2016).

The influence of the underlying stiff layer on the penetration resistance has also been investigated in cone penetration tests (CPT). Numerical analyses and field test data have shown that the strength and stiffness of underlying layers has an effect on the resistance in overlying layers (Van Den Berg et al., 1996; Lunne et al., 1997; Ahmadi and Robertson, 2005). The comparisons in Figure 8 suggest that the geometry, strength and/or stiffness of the underlying layer have impacts on the depth of deviation d_d from the bearing capacity solutions for jack-up foundations in top clay layer as a single layer.

To address the above shortcomings of Equation 28, an empirical formula is proposed below to predict the depth of transition d_t:

$$\frac{d_t}{D} = 0.11\frac{H_{ct}}{D} + 0.77\sqrt{\frac{H_s}{D}\left(\frac{\varphi' - \varphi_{cv}}{\varphi_{cv}}\right)} \quad ; \quad \frac{d_{tip}}{D} \le \frac{d_t}{D} \le \text{Min}\left(\left(\frac{H_{ct}}{D}\right), 0.70\right) \qquad 29$$

The first term approximates the effect of the top clay layer geometry whilst the second term approximates the effect of the sand layer geometry and strength properties. The expression in Equation 29 was calibrated using the centrifuge test data for sand layers with three relative densities of I_D = 51%, 74% and 89%. The operative friction angle φ' can be obtained from the iterative peak resistance calculations (Equations 17 and 23-25). Hence, the stress-dependent characteristic of sand is taken into account.

The lower bound on d_t/D in Equation 29 is to ensure that the spudcan can sense the underlying sand layer as soon as the tip touches the sand. The upper bound is to ensure that d_t/D does not exceed H_{ct}/D and the maximum value of 0.70 for a rigid boundary. The maximum value of d_t/D = 0.70 was derived using LDFE (large deformation finite element) analyses in Ullah et al. (2014) and agrees well with the solution of ~ 0.71 by Mandel and Salencon (1969), using the method of characteristics.

A graphical representation of Equation 29 is displayed in Figure 9 for $H_s/D = 0.75$. The effects of clay and sand layer geometry and sand strength properties on d_t/D are illustrated for a spudcan with $d_{tip}/D = 0.23$ (typical of Marathon Le Tourneau spudcan widely modelled at UWA; see Menzies and Roper, 2008 for an illustration of the geometry) and a flat foundation (where $d_{tip}/D = 0$). In general, d_t increases with increasing H_{ct}/D and $(\varphi'-\varphi_{cv})/\varphi_{cv}$. The range of d_t is greater for a flat footing than for a spudcan with conical underside due to the bounds in Equation 29.

After d_t is estimated, the depth of deviation from the mudline d_d can be calculated as:

$$d_d = H_{ct} - d_t \geq 0 \quad (30)$$

The performance verification of Equation 30 can be found later in the section where the spudcan full penetration profiles from centrifuge tests and from the proposed framework predictions are compared.

Once the peak resistance (q_{peak}), depth of peak resistance (d_{peak}) and depth of deviation (d_d) have been calculated, the penetration resistance profile in the top clay layer ($q_{clay\text{-}ct}$) can be estimated as follows:

1. Calculate the penetration resistance profile in the top clay layer ($q_{clay\text{-}ct}$) over the range of $0 \leq d \leq d_d$ using Equation 27 with N_c from Houlsby and Martin (2003).
2. Construct a straight line between the penetration resistance at deviation q_d (which occurs at the depth of deviation d_d) to the peak resistance q_{peak} (which occurs at the depth of peak resistance d_{peak}).

This procedure is much simpler than that of squeezing mechanism suggested by ISO (2012). At the same time, it provides better predictions of spudcan penetration resistance when compared with centrifuge data. More demonstrations of comparison can be found later in the full penetration profile section.

6.2 Penetration resistance estimation in the bottom clay layer ($q_{clay\text{-}cb}$)

Ullah et al. (2016)'s centrifuge experiments used image analysis to reveal that a small clay plug and a substantial sand plug become entrapped beneath jack-up footings following penetration through the sand layer (see Ullah et al., 2016). The proportion of the entrapped plug that

consisted of sand was very similar in size to that entrapped beneath similar foundations in two-layer sand-clay punch-through failure experiments reported by both Teh et al. (2008) and Hu et al. (2014b), with an average height of $0.9H_s/D$. Therefore, the following formula is proposed to estimate the height of the composite plug H_{plug} for clay-sand-clay stratigraphies as:

$$H_{plug} = 0.9H_s + H_c \quad (31)$$

where H_c is as defined earlier at $0.07H_{ct}$. The height of the composite foundation H_{fdn} is then expressed as:

$$H_{fdn} = H_{plug} + t \quad (32)$$

Where, t is the thickness of the foundation. For spudcan, t is the thickness of the shoulder.

The resistance in the bottom clay layer is then expressed as:

$$q_{clay-cb} = N_c s_u + H_{fdn}\gamma'_{cb} \quad (33)$$

The first term represents the resistance from the soil whilst the second term represents the buoyancy of the displaced soil. N_c is the deep bearing capacity factor, s_u is the undrained shear strength at the load reference point (LRP) on the foundation and γ'_{cb} is the effective unit weight of the bottom clay layer.

The following semi-empirical expression for N_c (calibrated from measured resistances at 0.5D penetration into the bottom clay layer) in the underlying clay layer in clay-sand-clay stratigraphies is proposed:

$$N_c = 0.55\frac{H_{ct}}{D} + 11\frac{H_s}{D} + 10.5 \quad (34)$$

The N_c factor is strongly proportional to the H_s/D ratio and slightly augmented by the H_{ct}/D ratio because the sand layer provides a greater proportion of the entrapped plug volume than the upper clay layer. For a purely sand over clay case (where $H_{ct}/D = 0$), Equation 34 simplifies that proposed by Hu et al., (2015c) for sand-clay stratigraphies, thus like the q_{peak} model proposed earlier in this paper, the penetration resistance in the underlying clay can be evaluated

for both clay-sand-clay as well as sand-clay stratigraphies using Equations 33 and 34 by setting $H_{ct}/D = 0$ where appropriate.

Hu et al. (2015c) found that the sand relative density (I_D = 43-99%) and the angle of the underside of the spudcan (θ_b = 0-21°) has no systematic impact on N_c for sand-clay stratigraphies and similarly no significant trends were observed in the experiments reported by Ullah et al. (2016) for clay-sand-clay stratigraphies. To account for potential variability of soil properties with depth, it was recommended by Hu et al. (2015c), that $N_c \pm 1\sigma$ be used to generate upper and lower bounds on the penetration resistance in the underlying clay layer from the best estimate soil strength, where σ is the standard deviation from the mean N_c, which for the experiments reported here is 1.73.

6.3 Summary of the full penetration resistance profile prediction method

A simplified prediction model for the full penetration resistance profile of spudcan on clay-sand-clay stratigraphies can be idealised by four linear segments, as illustrated schematically in Figure 10. The flow chart in Figure 11 outlines the calculations required to generate an estimate of the full penetration resistance profile illustrated in Figure 10.

This prediction method follows neither the 'top-down' approach nor 'bottom-up' approaches recommended in the industry guidelines (ISO, 2012) because the operative friction of the sand layer at peak resistances contributes to both the peak penetration resistance (q_{peak}) and penetration resistance in the top clay layer ($q_{clay\text{-}ct}$), so the peak resistance must be calculated first. The four calculation points capture the key parameters in a punch-through assessment – the peak resistance (which should not be exceeded by the leg load if the punch through distance is unacceptably large), and the punch through distance.

For sand-clay stratigraphies the penetration profile prediction approach is identical except that the top clay layer height H_{ct} is set to zero and the coordinate (q_{peak}, d_{peak}) is connected to the coordinate (0, $-d_{spg}$), where d_{spg} is the height of the spigot (i.e. d_{spg} is 0 for flat foundation).

7. PERFORMANCE OF FULL RESISTANCE PROFILE MODEL

Figure 12 demonstrates the performance of the model in predicting the penetration resistance measured in three selected centrifuge experiments modelling punch-through of jack-up

foundations: two for clay-sand-clay with dense and medium dense sand layers and one for dense sand overlying clay.

Solutions generated using the ISO (2012) recommendations are shown alongside. The punching-shear approach was used to predict the peak resistance q_{peak}. The penetration resistance in the top clay was calculated using the relations provided in Houlsby and Martin (2003) in conjunction with the squeezing model of Meyerhof and Chaplin (1953) when the criterion in Equation 28 was satisfied. The penetration resistance in the bottom clay layer was also estimated using N_c values after Houlsby and Martin (2003) thereby ignoring the presence of the entrapped plug of soil beneath the foundation as the ISO (2012) recommendations make no specific provision to account for any entrapped material beneath the foundation following punch-through.

A number of observations are drawn from these three comparisons:

1. The ISO (2012) calculations under-predict the penetration resistance, both in the prediction of q_{peak} and $q_{clay\text{-}cb}$, which fortuitously results in quite acceptable predictions for the potential punch-through depth, d_{punch} (see for instance Figure 12a test T3SP, which is marked in blue in Figures 6, 13 and 14 to highlight this phenomena).
2. The proposed approach yields similar predictions for the potential punch-through depth, d_{punch}, but as a product of much more accurate predictions of q_{peak} and $q_{clay\text{-}cb}$ than the ISO (2012) calculations, providing confidence in the various stages of the penetration resistance profile calculation. This greater accuracy raises the predicted maximum tolerable leg load without causing punch through, compared to the ISO method.
3. The linear simplifications employed by the model to approximate the transitions from q_{peak} to $q_{clay\text{-}cb}$ tend to underestimate the penetration resistance during punch-through. This is desirable as it provides a worst-case interpretation of the penetration resistance profile during punch-through. A more detailed increment-by-increment assessment could be performed using the same methodology, leading to a modest increase in realism.
4. The performance of the model for sand-clay stratigraphies is comparable to that for clay-sand-clay stratigraphies. This was expected because when $H_{ct} = 0$, the penetration

resistance profile model simplifies to the sand-clay model proposed and verified – experimentally and numerically – by Hu et al. (2015b,c).

Performance assessments for all the tests of Ullah et al. (2016) are available in the supplementary data.

Figure 13 presents a comparison of the value of N_c measured (by dividing the net penetration resistance q_{net} by the strength at that depth measured using a T-bar; see Ullah et al. 2016) and back-calculated using Equation 33 at the depth at which $q_{clay\text{-}cb}$ was equal to q_{peak} for each experiment (i.e. the depth at which punch-through failure would cease). The industrial guidelines of ISO (2012) and SNAME (2008) consistently under predict N_c in the bottom clay layer because they do not account for soil plug entrapment, which has been observed in image analysis (Ullah et al., 2016).

Two variants of N_c, one explicitly neglecting and one considering additional shear resistance along the trapped plug, was considered in the extended method of Teh (2007) (Figure 13e), given in Equation 35 and 37 respectively:

$$N_c = \frac{\left(q_{clay-cb} - \frac{4V_f}{\pi D^2}\gamma'_{cb} \right)}{s_{u(base)}} \quad 35$$

where $s_{u(base)}$ is the undrained shear strength at the base of the soil plug and $q_{clay\text{-}cb}$ as in Teh (2007) is given as:

$$q_{clay-cb} = N_c s_{u(base)} + \frac{4 s_{ua} \alpha_{side} H_{fdn}}{D} + \frac{4V_f}{\pi D^2}\gamma'_{cb} \quad 36$$

where s_{ua} is the average strength within the depth of the soil plug, α_{side} represents the side sand-clay interface adhesion factor assumed as unity and N_c is adopted from Hossain et al. (2006):

$$N_c = 10\left(1 + 0.075 \frac{d + H_{plug}}{D} \right) \leq 11.5 \quad 37$$

Teh's (2007) extended approach similarly does not capture the range in N_c measured due to the volume of soil entrapment beneath the foundation. In contrast the proposed approach performs reasonably well in predicting the experimental measurements with no systematic bias evident.

Although the measurements are somewhat scattered about the mean, both the standard deviation and COV are lower than the other methods.

Figure 14 presents a comparison of the measured and predicted punch-through depth d_{punch} for each of the experiments. Somewhat surprisingly, the industrial guidelines generate very good predictions for d_{punch}, however, it should be stressed that this is fortuitously a product of conservative predictions for both q_{peak} and $q_{clay\text{-}cb}$.

The extended version of Teh's (2007) approach performs better than the ISO (2012) approaches. However, ~26% of the predictions indicated no risk of punch-through even though punch-through occurred in the experiments and there is significant scatter in the predictions, as reflected by the mean, SD and COV of predicted over measured d_{punch} ratio (Figure 14e). By correctly modelling stress dependency of the sand layer in q_{peak} calculations and by considering the enhancement of N_c (due to soil plug entrapment) in the underlying clay layer-lead to excellent predictions of d_{punch}. The majority of the tests predict d_{punch} with values mostly within ±25% variation with a mean predicted over measured d_{punch} ratio of unity and relatively low SD and COV (Figure 14f).

The performance of the proposed approach has been verified by comparison of the predictions to measurements from 30 centrifuge model tests. The comparisons indicate that the proposed approach is superior to adaptations of the industry guidelines and other models for clay-sand-clay scenarios. The approach is simple and formulated in terms of meaningful physical parameters that can be defined by performing standard in-situ tests making the model well suited for performing routine punch-through assessment for locations with clay-sand-clay or sand-clay stratigraphies.

8. CONCLUSIONS

An analytical approach has been proposed to allow routine assessment of punch-through risk for jack-up rig foundations in clay-sand-clay stratigraphies. The method allows the spudcan peak resistance and the potential punch-through depth to be estimated more accurately. The method extended the current failure stress dependent models for sand-clay stratigraphies (Lee et al. 2013b, Hu et al. 2014a) to three layer clay-sand-clay soils. The model proposed was validated against 30 centrifuge model test results. The model performance was compared with

those generated by interpretations of the current industry guidelines (ISO, 2012). The following conclusions are obtained:

1. An extension of the failure stress-dependent model for the peak penetration resistance q_{peak} in the sand layer during punch-through for sand-clay stratigraphies (see Lee et al. 2013b; Hu et al. 2014a) has resulted in a universal model for q_{peak} that is suitable for generating predictions for both sand-clay and clay-sand-clay scenarios. The extended model performs very well in predicting q_{peak} for both sand-clay and clay-sand-clay cases for the geometries and soil properties tested in this pair of companion papers. There is less bias and scatter than the other methods considered in the performance comparison.
2. Similarly, a very simple semi-empirical extension of the bearing capacity model for the underlying clay layer following punch-through (Hu et al. 2014b) has been proposed that performs equally well for sand-clay or clay-sand-clay scenarios, for the geometries and soil properties tested in this pair of companion papers. Prediction of the penetration resistance in the underlying clay layer q_{clay} and the peak resistance q_{peak} allows the potential punch-through depth to be estimated. The proposed approach implicitly accounts for the change in bearing capacity factor mobilised for different entrapped soil plug geometries; a feature that is not captured by current industry guidelines.
3. The combination of the calculations referred to in 1 and 2 above results in good predictions of the punch-through depth d_{punch}. Critically, the proposed method captures more accurately the punch-through risk than the current industry guidelines or alternative recommendations, as well as being more accurate in predicting q_{peak} thus raising the allowable leg load range in for the conditions considered in this study.
4. The penetration resistance preceding peak resistance has been approximated using an alternative semi-empirical approach to the squeezing model recommended in the industry guidelines. This model accounts for the geometry of the layers and their strength leading to more accurate estimation of the depth of transition from classical shallow bearing capacity to punch-though failure than current industry recommendations. In addition, this relation is appropriately bounded to account for spudcan underside geometry leading to early sensing of the stiff underlying boundary, which precludes ‘squeezing-type’ mechanisms.

5. The models were developed with the aid of PIV observations derived from model tests using one spudcan and flat footing diameter (6 m in prototype terms) in medium dense to dense sand interbedded in clay (Ullah et al. 2016). Although, the models yield excellent predictions for foundations with prototype diameters in the range of 6 m to 16 m, there is potential for further refinement (particularly the fitting parameters f_1 and f_2 for example) in the future through further centrifuge tests, or ideally from field observations.
6. The models developed can be applied to both clay-sand-clay and sand-clay stratigraphies. All steps are expressed analytically, making the approach easily coded into a spreadsheet or other software for routine use.
7. All the parameters required to estimate the penetration resistance profile have clear physical meaning and can be obtained from existing laboratory tests.

9. ACKNOWLEDGEMENTS

The research presented here forms part of the activities of the Centre for Offshore Foundation Systems (COFS), currently supported as a node of the Australian Research Council Centre of Excellence for Geotechnical Science and Engineering (grant CE110001009) and through the Fugro Chair in Geotechnics, the Lloyd's Register Foundation Chair and Centre of Excellence in Offshore Foundations and the Shell EMI Chair in Offshore Engineering (held by the fourth author). The authors would like to acknowledge the financial contribution of the Australian Research Council (ARC) through Discovery Project DP1096764.

10. REFERENCES

Ahmadi, M. M. & Robertson, P. K. (2005). Thin-layer effects on the CPT qc measurement. *Canadian Geotechnical Journal* **42(5)**:1302-1317.

Baglioni, V. P., Chow, G. S. & Endley, S. N. (1982). Jack-up rig foundation stability in stratified soil profiles. In *Proceedings of Offshore Technology Conference*, OTC 4409, pp. 363-384.

Bolton, M. D. (1986). The strength and dilitancy of sands. *Géotechnique* **36(1)**:65-78.

Dier, A., Carroll, B. & Abolfathi, S. (2004). Guidelines for jack-up rigs with particular reference to foundation integrity. Health and Safety Executive (HSE), Research report 289, UK, pp. 1-91.

Drescher, A. & Detournay, E. (1993). Limit load in translational failure mechanisms for associative and non-associative materials. *Géotechnique* **43(3)**:443-456.

Dutt, R. N. & Ingram, W. B. (1984). Jackup rig siting in calcareous soils. In *Proceedings of*. Offshore Technology Conference, OTC 4840, pp. 541-548.

Hansen, J. B. (1970). *A revised and extended formula for bearing capacity. Bulleting of the Danish Geotechnical Institute,28,5-11*.

Hossain, M. S., Randolph, M. F., Hu, Y. & White, D. J. (2006). Cavity stability and bearing capacity of spudcan foundations on clay. In *Proceedings of Offshore Technology Conference*, OTC 17770, pp. 1-18.

Hossain, M. S. (2014). Experimental investigation of spudcan penetration in multi-layer clays with interbedded sand layers. *Géotechnique* **64(4)**:258-276.

Hossain, M. S. & Randolph, M. F. (2009) New mechanism based design approach for spudcan foundations on single layer clay. *Journal of geotechnical and geoenvironmental engineering,ASCE* **135(9)**, 1264-1274.

Houlsby, G. T. & Martin, C. M. (2003.) Undrained bearing capacity factors for conical footings on clay. *Géotechnique* **53(5)**:513-520.

Hu, P., Stanier, S. A., Cassidy, M. J. & Wang, D. (2014a). Predicting peak resistance of spudcan penetrating sand overlying clay. *Journal of Geotechnical and Geoenvironmental Engineering* **140(2)**:04013009.

Hu, P., Wang, D., Cassidy, M. J. & Stanier, S. A. (2014b). Predicting the resistance profile of a spudcan penetrating sand overlying clay. *Canadian Geotechnical Journal* **51**:1151-1164.

Hu, P., Stanier, S. A., Wang, D. & Cassidy, M. J. (2015a). A comparison of full profile prediction methods for a spudcan penetrating sand overlying clay. *Géotechnique Letters* **5(3)**:131-139.

Hu, P., Stanier, S. A., Wang, D. & Cassidy, M. J. (2015b). Effect of footing shape on penetration in sand overlying clay. *International Journal of Physical Modelling in Geotechnics* **16(3)**:119-133.

Hu, P., Wang, D., Stanier, S. A. & Cassidy, M. J. (2015c). Assessing the punch-through hazard of a spudcan on sand overlying clay. *Géotechnique* **65(11)**:883-896.

ISO (2012). 19905-1: Petroleum and natural gas industries- site specific assessment of mobile offshore units-Part 1 : Jack-ups. Geneva, Switzerland : International Organization for Standardization.

Lee, K. K., Cassidy, M. J. & Randolph, M. F. (2013a). Bearing capacity on sand overlying clay soils: experimental and finite-element investigation of potential punch-through failure. *Géotechnique* **63(15)**:1271-1284.

Lee, K. K., Randolph, M. F. & Cassidy, M. J. (2013b). Bearing capacity on sand overlying clay soils: a simplified conceptual model. *Géotechnique* **63(15)**:1285-1297.

Lunne, T., Robertson, P. K. & Powell, J. M. (1997). *Cone penetration testing in geotechnical practice.* London, UK, Blackie Academic and Professional.

Mandel, J. & Salencon, J. (1969). The bearing capacity of soils on a rock foundation. In *7th International Conference on Soil Mechanics and Foundation Engineering*. Mexico, pp. 157-164.

Martin, C. M. (1994). Physical and numerical modelling of offshore foundations under combined loads. PhD thesis, University of Oxford.

Menzies, D. & Roper, R. (2008). Comparison of jackup rig spudcan penetration methods in clay. In *Offshore Technology Conference*. Houston, Texas, OTC 19545 pp. 1-22.

Meyerhof, G. G. & Chaplin , T. K. (1953). The compression and bearing capacity of cohesive layers. *British Journal of Applied Physics* **4(1)**:20-26.

Osborne, J. & Paisley, J. (2002). South east Asia jack-up punch-throughs: the way forward, *Proceedings of the conference on offshore site investigation and geotechnics - sustainability and diversity*, London, UK., pp. 301-306.

SNAME (2008):Recommended practice for site specific assessment of mobile jack-up units. T & R Bulletin 5-5A 1st edn, rev 3. Alexandria, VA, USA : Society of Naval Architechts and Marine Engineers.

Stanier, S.A., Blaber, J., Take W.A. & White, D.J. (2016). Improved image-based deformation measurement for geotechnical applications. Canadian Geotechnical Journal, DOI: 10.1139/cgj-2015-0253.

Teh, K.L., Leung, C.F., Chow, Y.K. & Handidjaja, P. (2009). Prediction of punch-through for spudcan penetration in sand overlying clay. In *Proceedings of Offshore Technology Conference*, OTC 20060, pp. 1-14.

Teh, K. L. (2007). Punch through of spudcan foundation on sand overlying clay. National University of Singapore, PhD thesis.

Teh, K. L., Cassidy, M. J., Leung, C. F., Chow, Y. K., Randolph, M. F. & Quah, C. K. (2008). Revealing the bearing capacity mechanisms of a penetrating spudcan through sand overlying clay. *Géotechnique* **58(10)**:793-804.

Teh, K. L., Leung, C. F., Chow, Y. K. & Cassidy, M. J. (2010). Centrifuge model study of spudcan penetration in sand overlying clay. *Géotechnique* **60(11)**:825-842.

Ullah, S. N., Hu, Y., White, D. & Stanier, S. (2014). LDFE study of bottom boundary effect in foundation model tests. *International Journal of Physical Modelling in Geotechnics* **14(3)**:80-87.

Ullah, S. N.,Stanier, S.A., Hu, Y. & White, D.J. (2016). Foundation punch-through in clay with sand: centrifuge modelling. *Géotechnique (submitted).*

Van Den Berg, P., De Borst, R. & Huétink, H. (1996). An eulerian finite element model for penetration in layered soil *International Journal for Numerical and Analytical Methods in Geomechanics* **20(12)**:865-886.

White D.J., Take W.A. & Bolton M.D. (2003). Soil deformation measurement using Particle Image Velocimetry (PIV) and photogrammetry. Géotechnique **53(7)**:619-631

Xie, Y., Falepin, H. & Jaeck, C. (2010) Prediction of spudcan penetration resistance in multiple soil layers. In *Proceedings of.* The International Society of Offshore and Polar Engineers, pp. 369-377.

NOTATIONS

A	Bearing area of circular foundation
A_{ls}	Lateral surface area of sand frustum
d	Foundation penetration depth
D	Foundation diameter
d_d	Depth of deviation from a single layer clay type response (measured from the mudline)
d_t	Depth of transition (measured from the top of sand)
d_{crit}	Peak mobilisation depth in the method of Teh
D_F	Distribution factor
d_{peak}	Depth of peak position
d_{punch}	Punch-through depth
d_{spg}	Height of spigot of spudcan foundation
E	Clay-Sand-Clay model parameter
f_1, f_2	Constant factors in the new conceptual model
H_c	Height of trapped clay
H_{ct}	Height of top clay
H_{eff}	Effective sand height
H_{fdn}	Height of composite foundation
H_{plug}	Height of soil plug under foundation
H_s	Height of sand
I_D	Sand relative density
I_R	Relative density index
K_p	Passive earth pressure coefficient
m	Bolton's parameter indicating contribution of dilatancy to sand strength

N_c	Clay bearing capacity factor
N_{co}	Bearing capacity factor due to cohesion at the base of a circular foundation
$N_{q,cone}$	Bearing capacity factor due to surcharge of a conical foundation
$N_{\gamma,cone}$	Bearing capacity factor due to weight of a conical foundation
p_o'	Mean effective stress
Q	Total bearing force under a foundation in Teh method
Q	Natural logarithm of grain crushing strength in kPa
Q_c	Clay bearing force at the sand clay interface in the method of Teh
q_{clay}	Bearing capacity in clay
$q_{clay-cb}$	Bottom clay bearing capacity
$q_{clay-ct}$	Bearing capacity in top clay
q_d	Bearing pressure at the depth of deviation
q_{nom}	Nominal bearing pressure
q_o	Surcharge
$q_{o(s)}$	Surcharge on top of sand in clay-sand-clay
q_{peak}	Peak bearing capacity
Q_s	Sand shearing force in the method of Teh
q_{sand}	Sand bearing capacity
R	Foundation radius
R, r	Geometric parameters in the method of Teh
s_u	Undrained shear strength of clay
s_{ubi}	Bottom sand clay intercept strength in clay-sand-clay

s_{um}	Undrained clay strength at mudline
t	Thickness of foundation
V_f	Volume of foundation
W	Weight of frustum in Teh method
W_{SF}	Weight of sand frustum
z	Vertical coordinate (downward positive)

Greek

γ'_s	Sand effective unit weight
γ'_{ct}	Top clay effective unit weight
γ'_{cb}	Bottom clay effective unit weight
θ	Skew angle
θ_b	Spudcan base angle with horizontal
κ	Strength non-homogeneity or normalised strength gradient
μ	Mean value
ρ_{ct}	Top clay undrained shear strength gradient
ρ_{bt}	Bottom clay undrained shear strength gradient
σ	Standard deviation
σ'_{hp}	Passive earth pressure
σ'_n	Normal effective stress acting on the sides of the sand frustum
σ'_z	Effective vertical stress within the sand frustum
τ_c	Shear stress at the periphery of trapped clay
τ_s	Shear stresses in sand
φ'	Operative friction angle
φ_{cv}	Constant volume friction angle

φ^*	Reduced operative friction angle
φ_2	Mean of the operative and constant volume friction angle in Teh method
ψ	Dilation angle
ψ_t	Geometric parameter representing the inclination of the slip surface in Teh method

Abbreviations

COV	Coefficient of variation
FE	Finite element
ISO	International Organization for Standardization
PIV	Particle image velocimetry
SD	Standard deviation
SNAME	The Society for Naval Architects and Marine Engineers
UWA	The University of Western Australia

11. LIST OF FIGURES

12. LIST OF TABLES

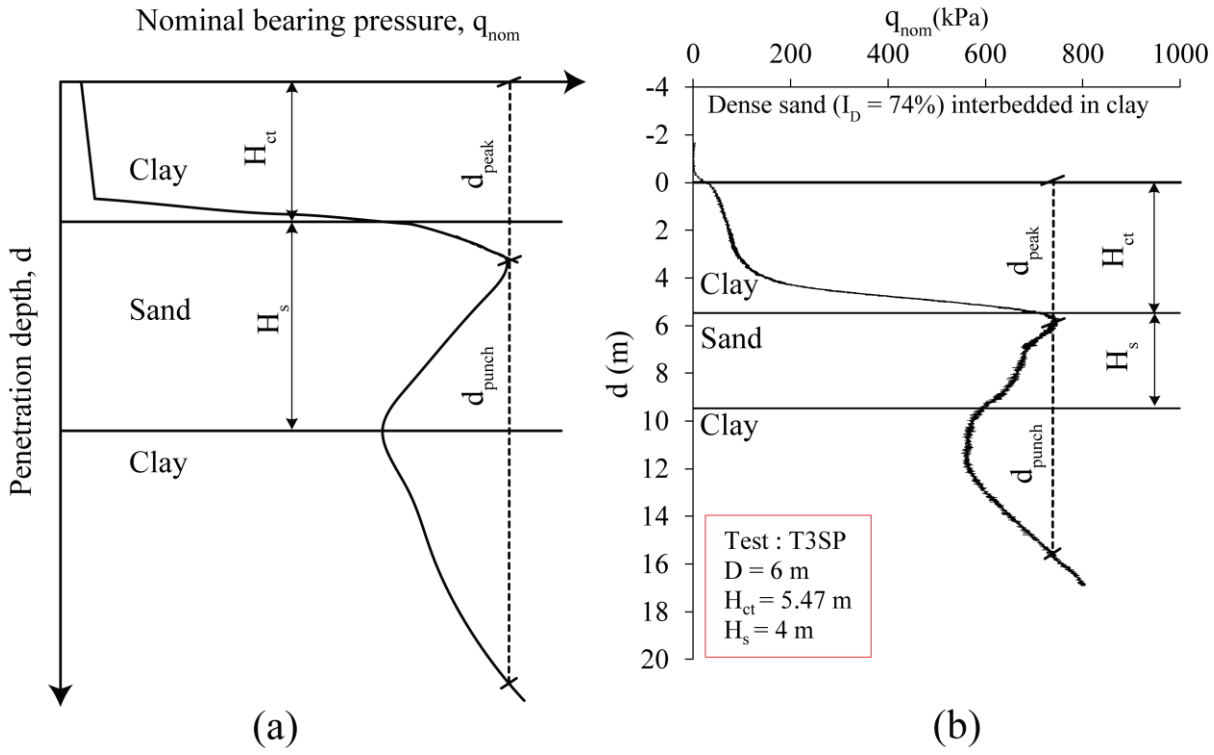

Figure 1: (a) Typical load-penetration response in clay-sand-clay stratigraphy and (b) centrifuge test data in clay-sand-clay after Ullah et al. (2016).

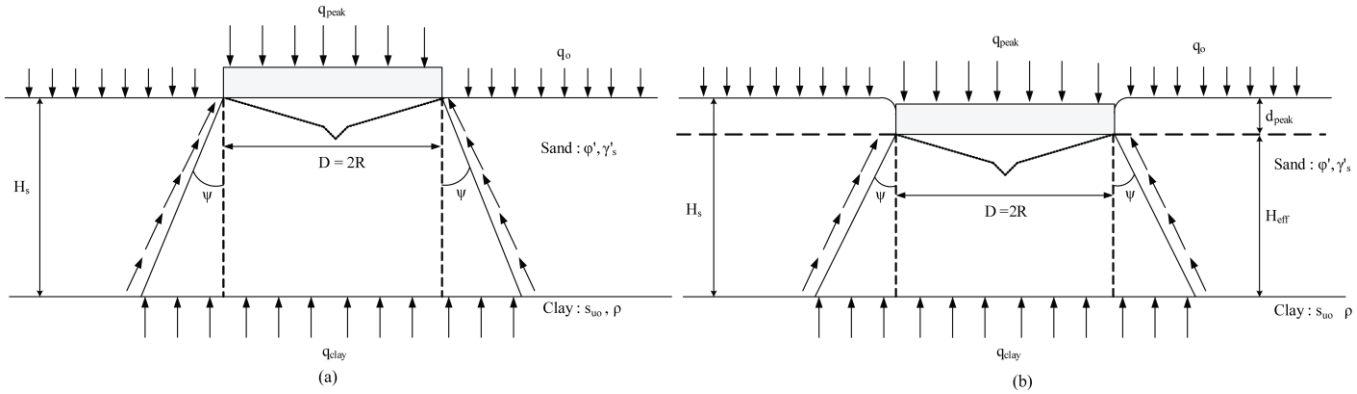

Figure 2: Recent analytical models of punch through on sand overlying clay: (a) mechanism of Lee et al. (2013b); (b) mechanism of Hu et al. (2014a).

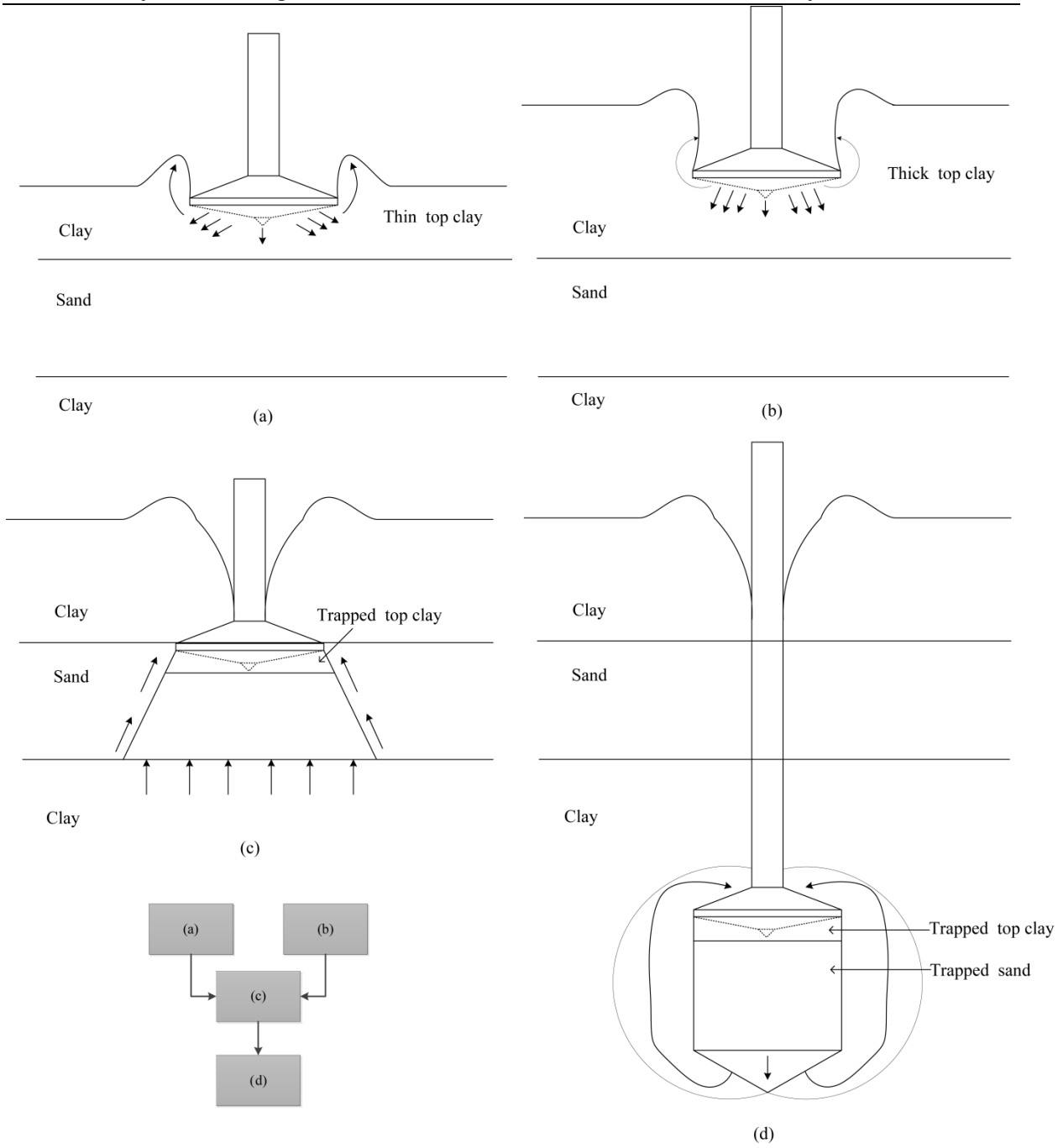

Figure 3: Summary of soil flow mechanisms in clay-sand-clay: (a) squeezing of thin clay layer; (b) bearing failure of thick clay layer; (c) peak resistance in sand layer; and (d) bearing capacity of the composite spudcan, clay and sand plug in the underlying clay layer.

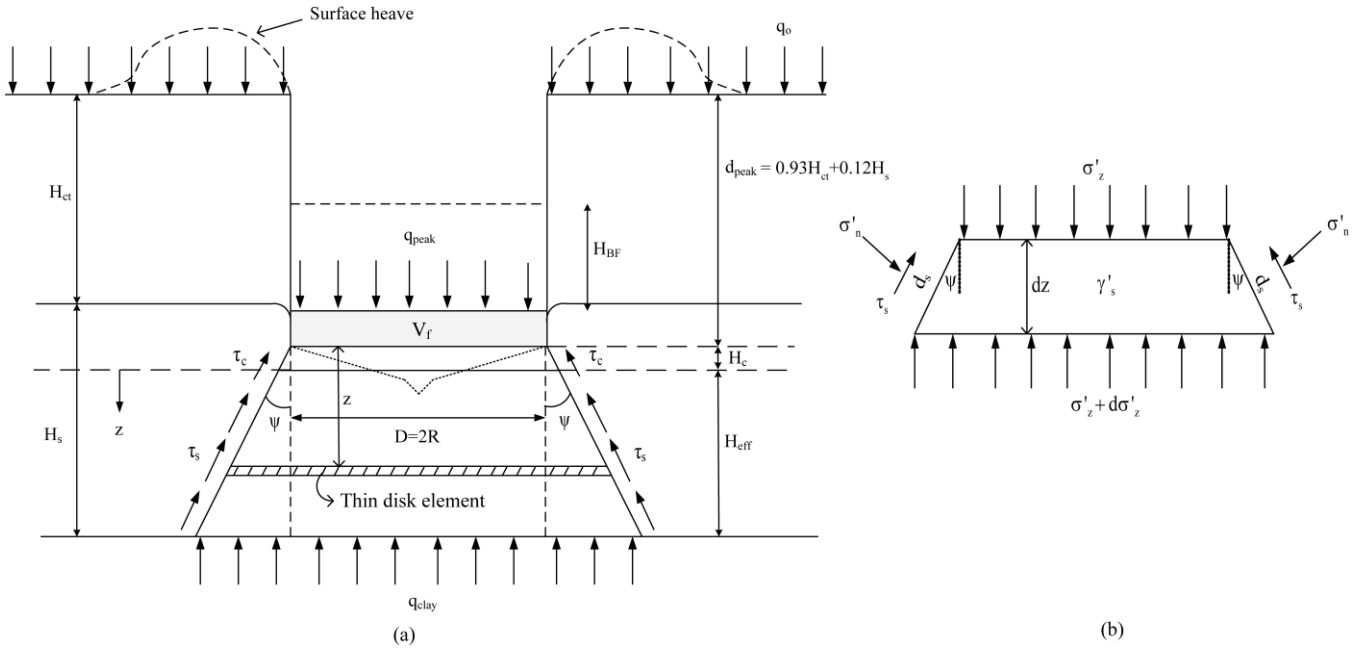

Figure 4: Peak resistance model: (a) idealised failure mechanism for clay-sand-clay stratigraphies; and (b) forces acting on an infinitesimally thin disk element.

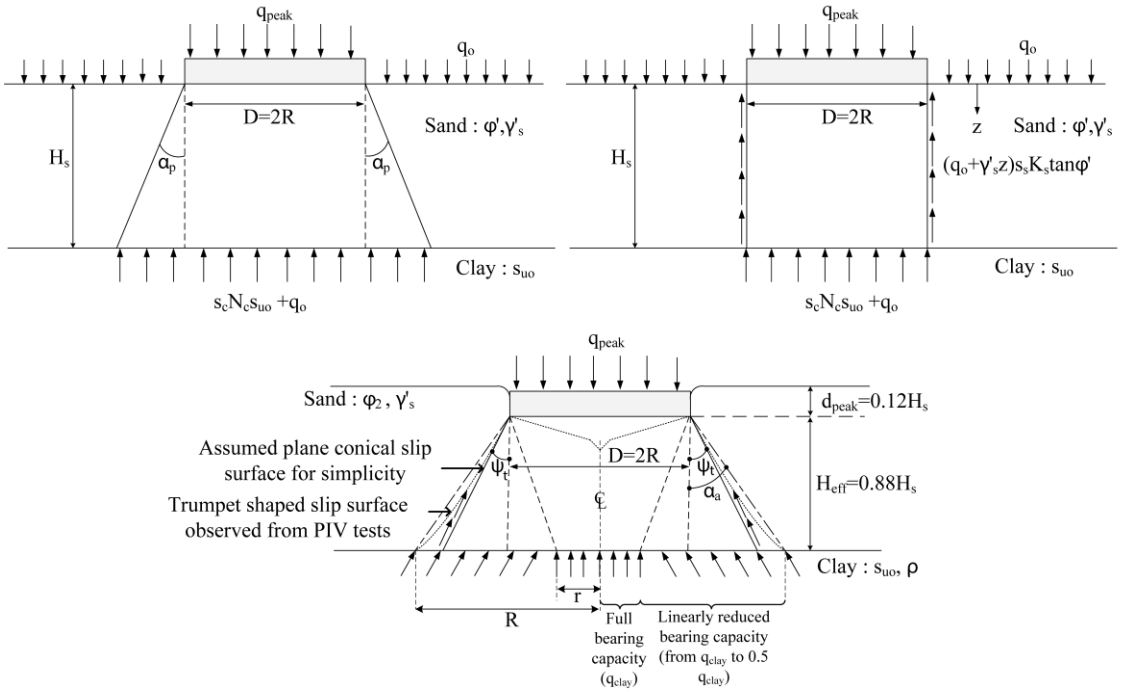

Figure 5: Schematics of: (a) the projected area (PA); (b) punching shear (PS); and (c) Teh's (2007) peak resistance mechanisms.

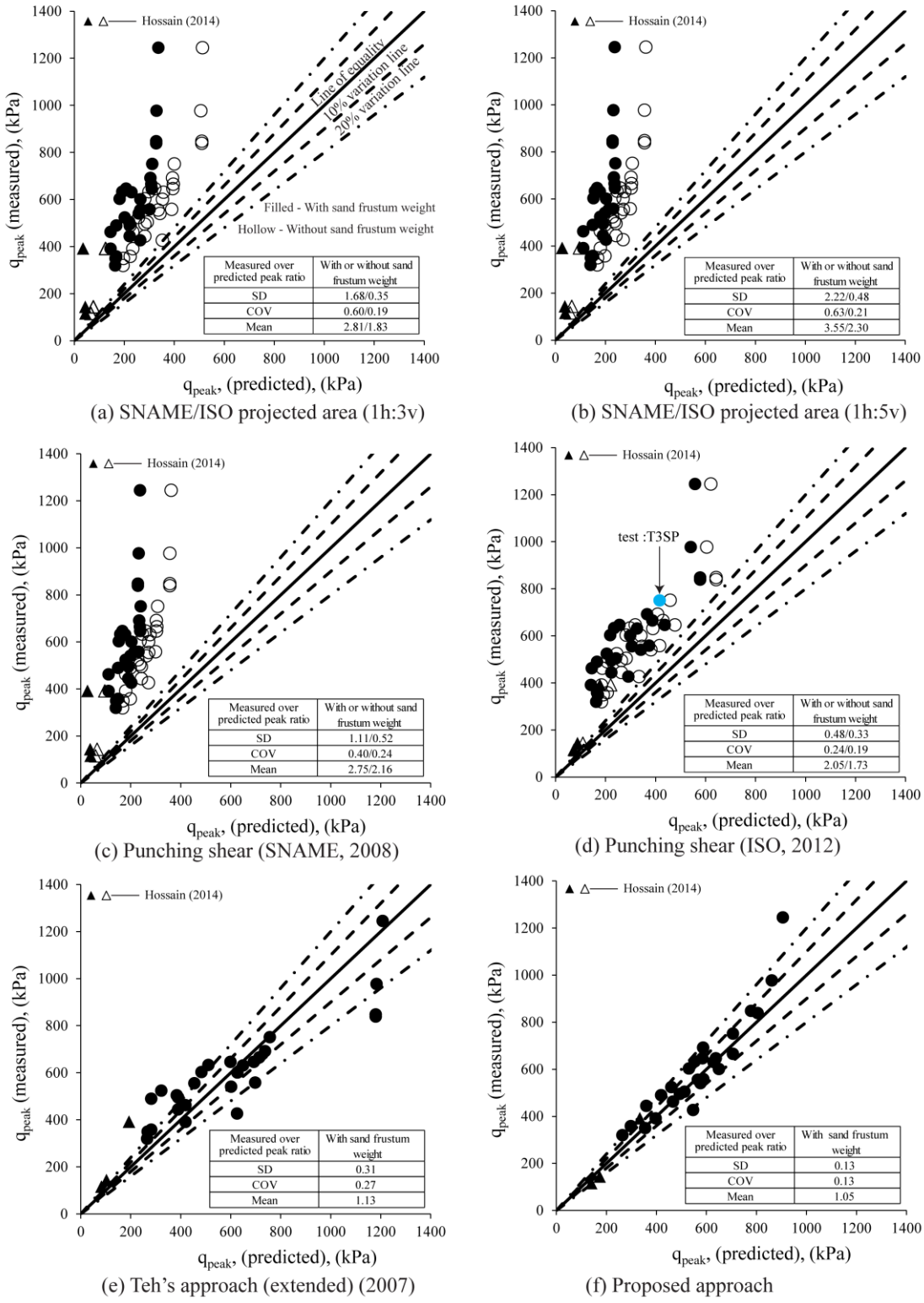

Figure 6: Observed performance in predicting the peak penetration resistance, q_{peak}: (a) Projected area or load spread (1h:3v); (b) projected area or load spread (1h:5v); (c) punching shear approach (SNAME, 2008); (d) punching shear approach (ISO, 2012); (e) extended Teh's (2007) approach; and (f) the proposed approach.

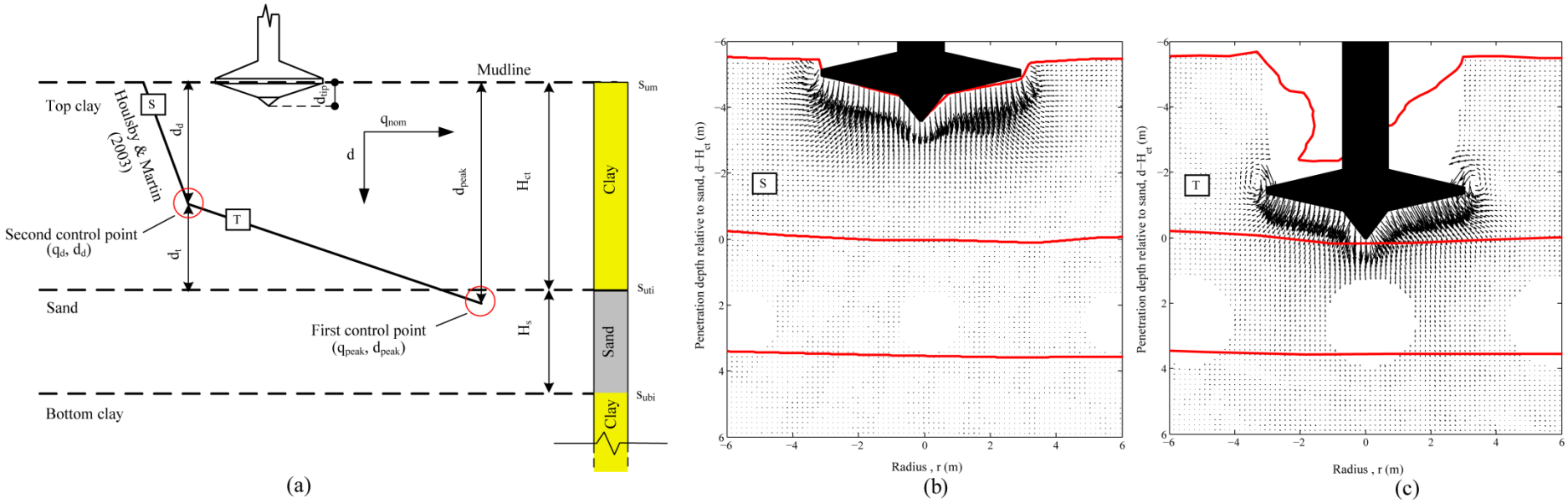

Figure 7: Top clay penetration resistance profile estimation: (a) diagram of key points in prediction; (b) soil flow mechanism prior to point of deviation; and (c) soil flow mechanism after point of deviation.

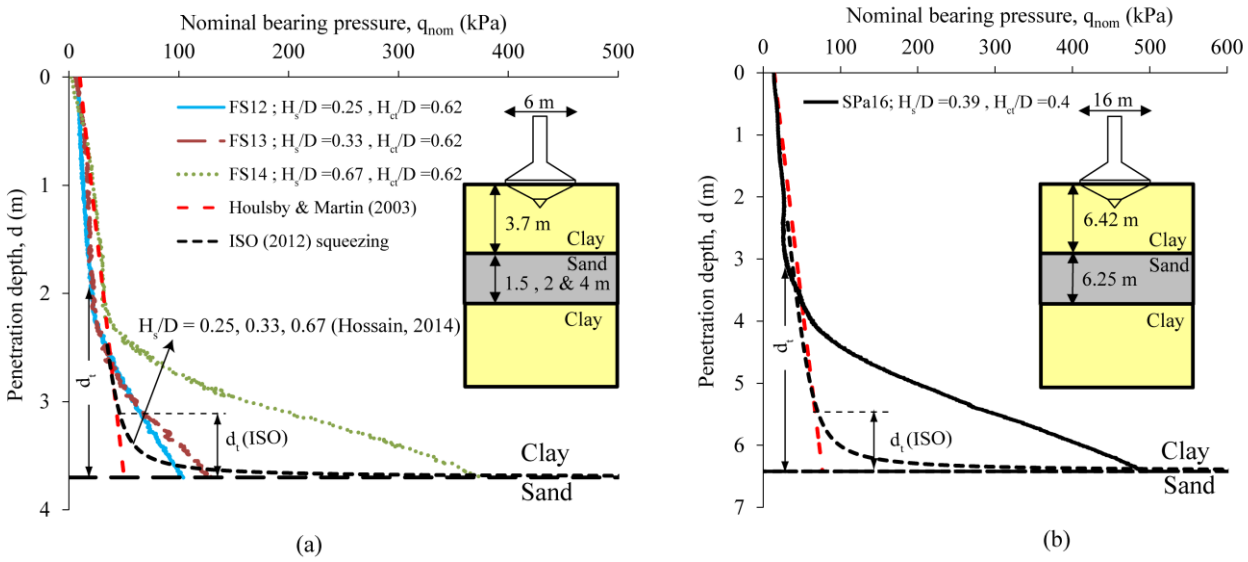

Figure 8: Comparison of ISO (2012) squeezing solution with centrifuge experiments from: (a) Hossain (2014); and (b) Ullah et al. (2016).

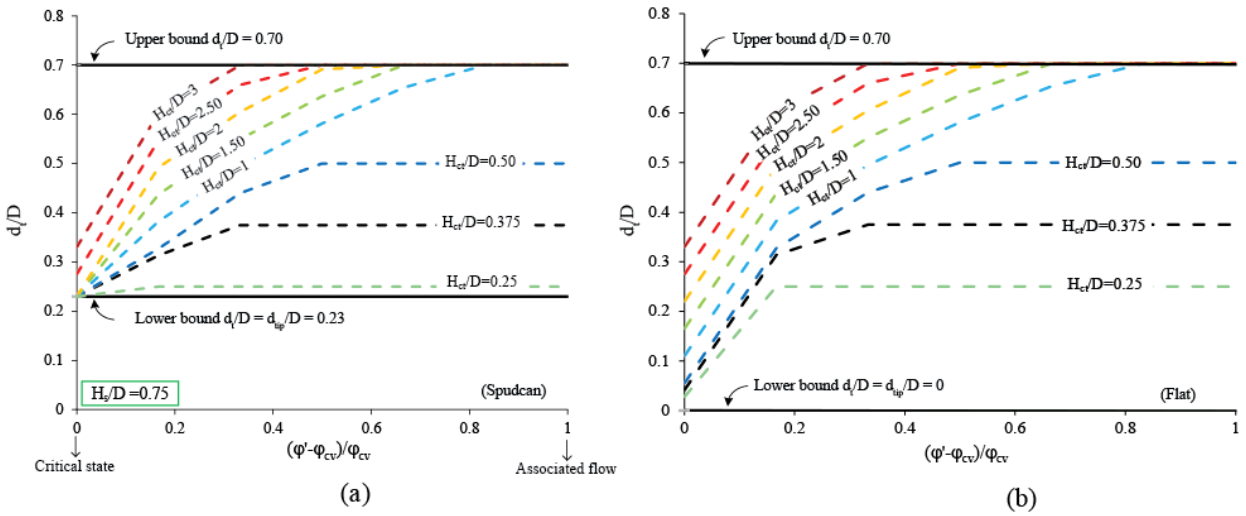

Figure 9: Nomogram of the depth of transition for H_s/D of 0.75: (a) a typical spudcan with spigot (or tip); and (b) a flat foundation.

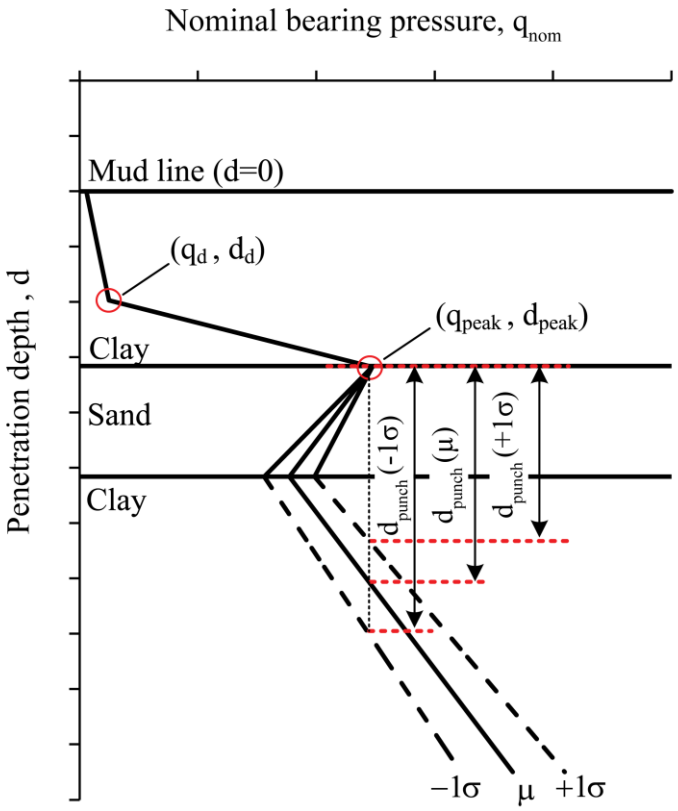

Figure 10: Schematic of the proposed full penetration resistance profile prediction method.

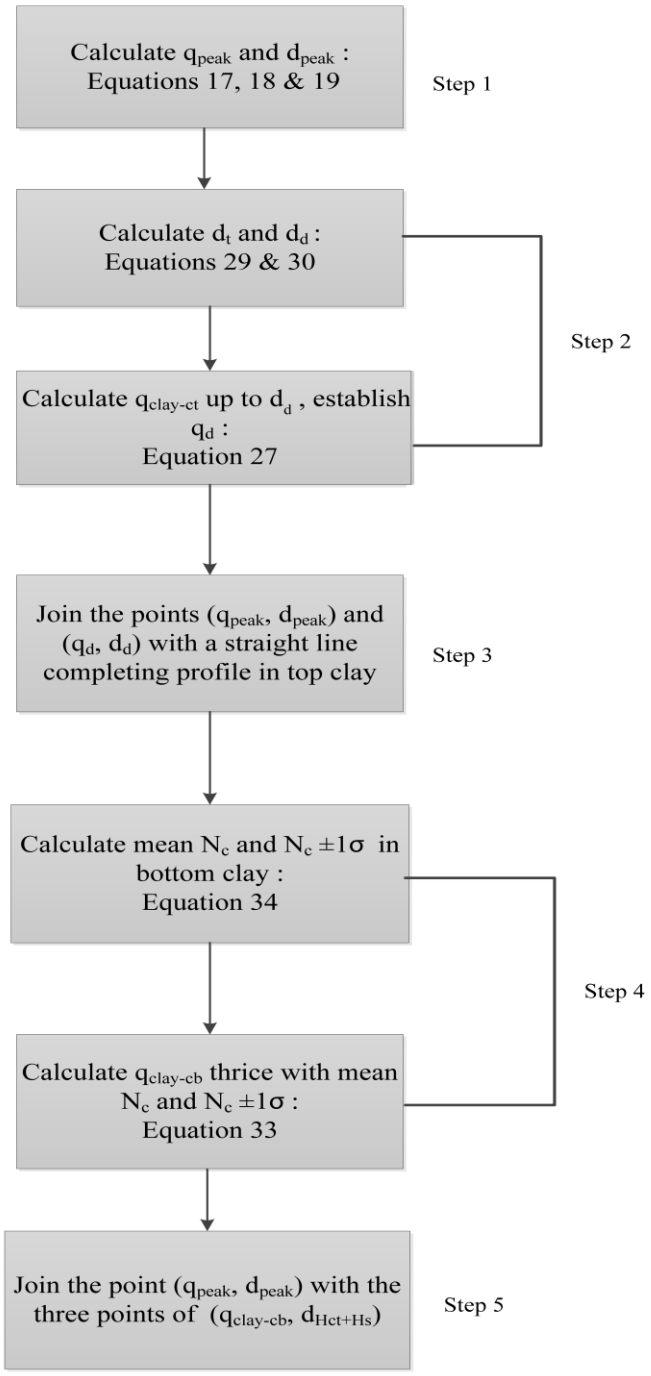

Figure 11: Flow chart for full penetration resistance profile prediction

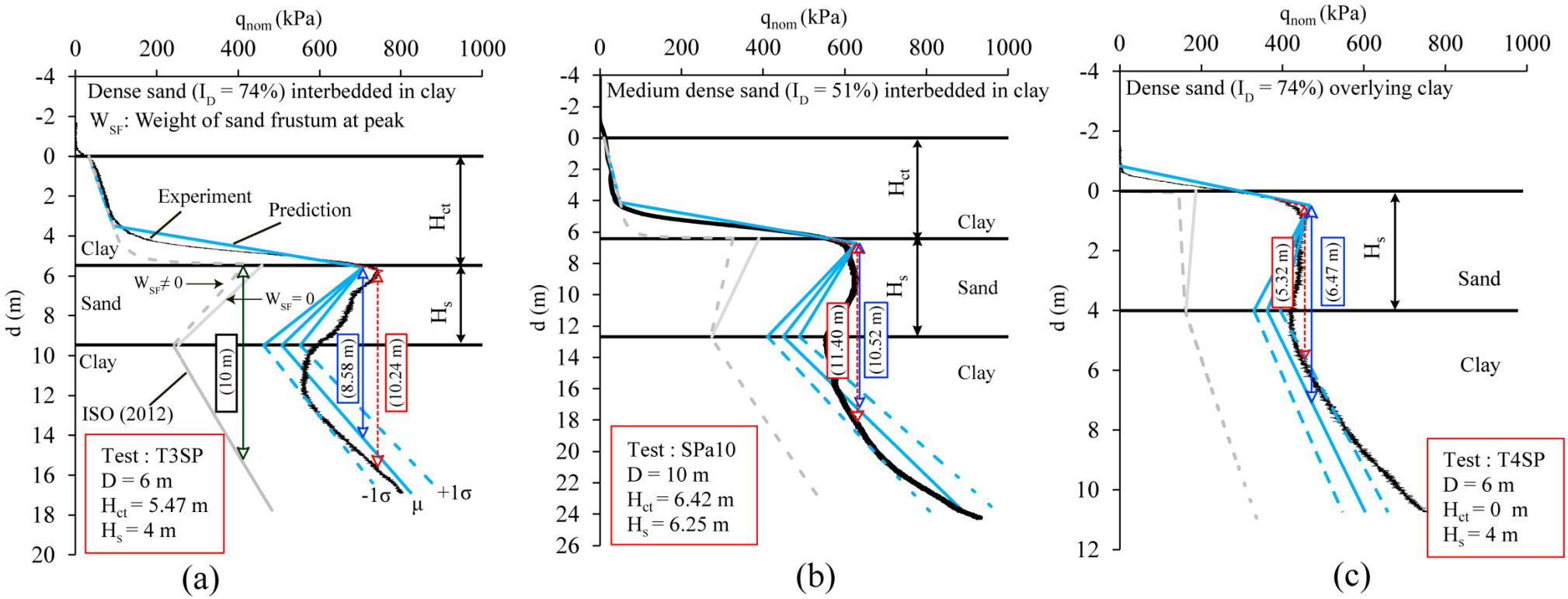

Figure 12: Prediction of complete penetration resistance profile on: (a) clay-sand-clay with a dense sand layer; (b) clay-sand-clay with a medium dense sand layer; and (c) dense sand overlying clay.

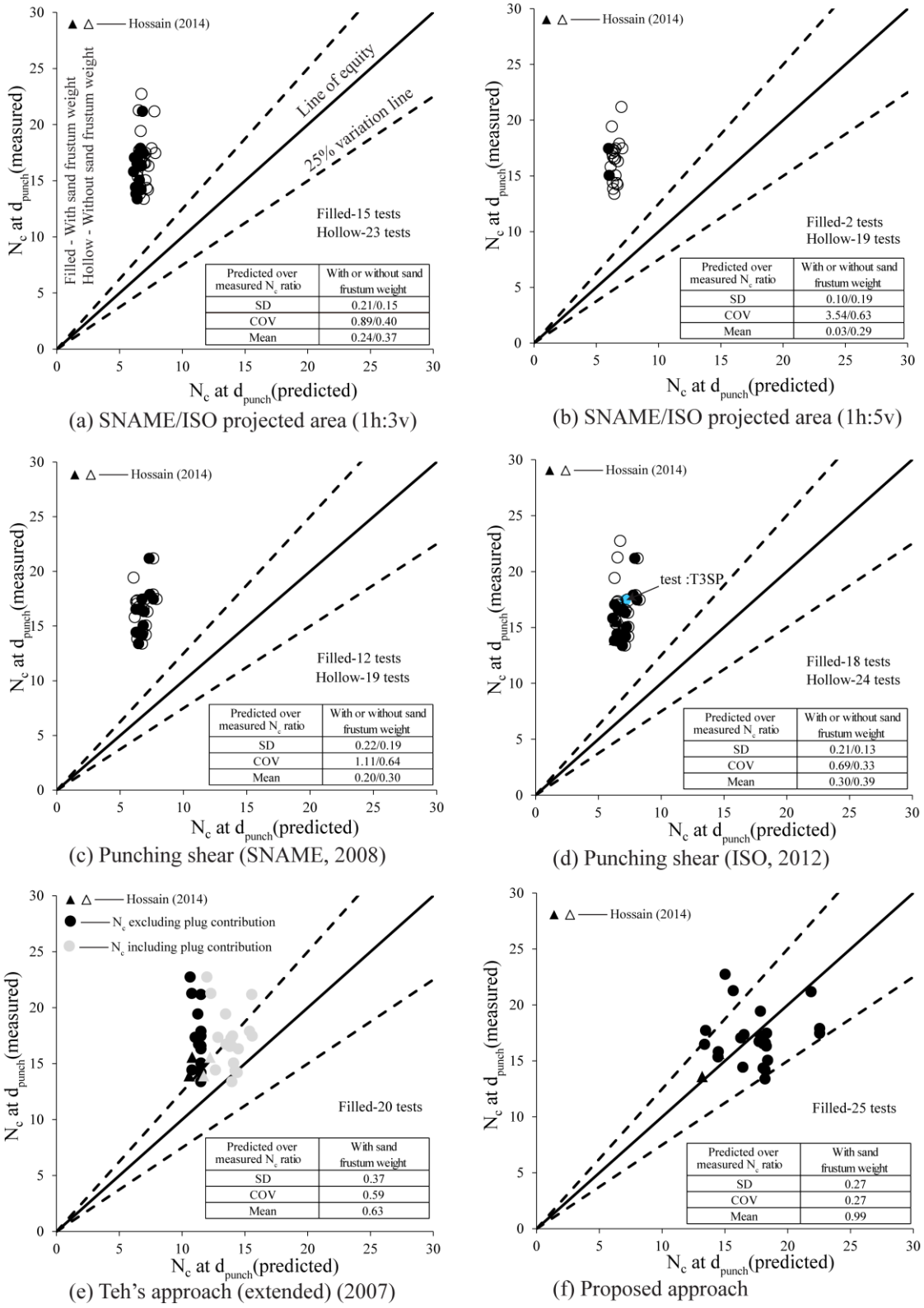

Figure 13: Predicted vs. measured back-calculated bearing capacity factor (N_c) in the underlying clay layer: (a) projected-area or load-spread (1h:3v); (b) projected-area or load-spread (1h:5v); (c) punching-shear approach (SNAME, 2008); (d) punching shear approach (ISO, 2012); (e) extended Teh's approach (2007); and (f) proposed approach.

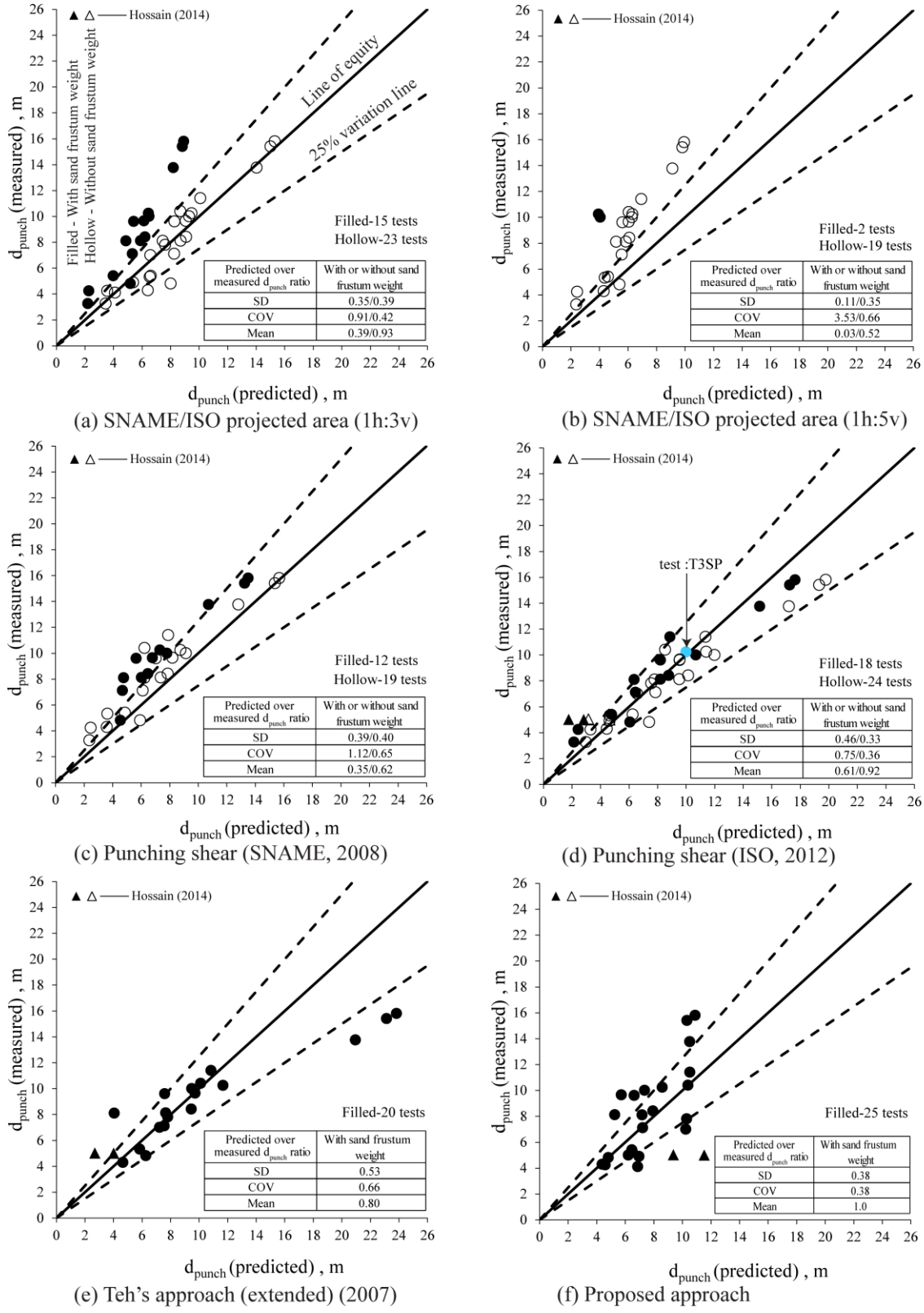

Figure 14: Performance in terms of predicting punch-through depth d_{punch}: (a) projected-area or load-spread (1h:3v); (b) projected-area or load-spread (1h:5v); (c) punching-shear approach (SNAME, 2008); (d) punching-shear approach (ISO, 2012); (e) extended Teh's approach (2007); and (f) proposed approach.

Table 1: Parameters required for predicting peak resistance q_{peak}.

Parameter category	Symbol	Description	Method of determining parameter
Foundation geometry	D & V_f	Foundation diameter and volume	Known parameters
Top clay	H_{ct}	Top clay height	Measured in situ
	H_c	Height of trapped clay	Taken as $f_1 H_{ct}$ with $f_1 = 0.07$.
	s_{um}	Mud line undrained shear strength	Measured in situ or in laboratory tests.
	ρ_{ct}	Top clay strength gradient	Measured in situ.
	γ'_{ct}	Top clay unit weight	Inferred from in situ tests or directly measured in the laboratory.
	f_1	Factor determining the amount of top clay	Taken as 0.07. Suggesting on average 7% of the top clay gets entrapped under the foundation.
	f_2	Factor determining the height of backfill	f_2 is taken as 0.50 (half backfill condition).
Sand	H_s	Sand height	Measured in situ.
	I_D	Sand relative density	Measured in the laboratory from undisturbed samples or in situ.
	Q	Parameter in Bolton (1986) equation	Measured from laboratory tests, For siliceous sand can be taken as 10.
	I_R	Relative density index	Obtained through an iterative procedure involving Equations 17, 23, 24 & 25.
	φ_{cv}	Constant volume friction angle	Measured from laboratory tests.
	φ' & ψ	Operative friction and dilation angle	Obtained from Equations 24 & 25 : $\varphi' = \varphi_{cv} + 2.65 I_R$ & $0.8\psi = \varphi' - \varphi_{cv}$, $\psi \geq 0$
	φ^*	Reduced friction angle due to non-associated flow of sand	Obtained from Equation 3 : $\tan\varphi^* = \frac{\sin\varphi'\cos\psi}{1-\sin\varphi'\sin\psi}$
	γ'_s	Effective unit weight of sand	Inferred from in situ tests or directly measured in the laboratory.
Bottom clay	s_{ubi}	Bottom sand-clay intercept strength	Measured in situ.
	ρ_{cb}	Bottom clay strength gradient	Measured in situ.
	κ	Non dimensional strength parameter needed to determine the bearing capacity factor from (Houlsby and Martin, 2003).	Calculated from Equation 11: $\kappa = \frac{\rho_{cb}\left\{D + 2\left(H_{eff} + H_c\right)\tan\psi\right\}}{s_{ubi}}$; H_{eff} is taken as $0.88H_s$.
	N_{co}	Bottom clay bearing capacity factor	Calculated from Equation 10: $N_{co} = 6.34 + 0.56\kappa$ (Houlsby and Martin, 2003)
Empirical factor	D_F	Distribution factor: Defined as the ratio of the normal effective stress at the slip surface to the mean vertical effective stress within the sand frustum.	For spudcan use Equation 6: $D_F(\text{spudcan}) = 0.642\left(\frac{H_s}{D}\right)^{-0.576}$; $0.16 \leq \frac{H_s}{D} \leq 1.0$ For flat foundation use Equation 7: $D_F(\text{flat}) = 0.623\left(\frac{H_s}{D}\right)^{-0.174}$; $0.21 < \frac{H_s}{D} < 1.12$

APPENDIX

1. EXTENDED TEH METHOD

The method of Teh (2007) is strictly applicable to sand over clay soils only, as no surcharge (q_o) term was considered while developing the model. However, for comparison purposes, the method is extended here to incorporate the effective surcharge ($q_o = H_{ct}\gamma'_{ct}$) as follows.

According to Teh (2007), the foundation peak resisting force (Q) from soil is given as:

$$Q = Q_s + Q_c - W \quad (1)$$

where, Q_s is the sand shearing resistance, Q_c is the resistance contribution from the bottom clay and W is the weight of the sand frustum. The effect of the additional surcharge is to increase the sand shearing resistance and the bottom clay bearing capacity. The weight of the sand frustum is unaffected by the presence of the surcharge q_o. The contribution of q_o on Q_s and Q_c are evaluated separately below.

Evaluating the sand shearing resistance, Q_s

Referring to Figure 1, Teh (2007) assumed that the stresses at the side of the sand frustum are in a passive state. Hence, if N is the total normal force acting on the side of the frustum and A_{ls} is the lateral surface area of the sand frustum, then the Rankine's effective passive earth pressure σ'_{hp} can be written as:

$$\sigma'_{hp} = \frac{dN}{dAls} = \gamma'_s K_p \left(d_{crit} + z\right) + q_o K_p \quad (2)$$

Where, K_p is the Rankine's passive earth pressure coefficient given as:

$$K_p = \frac{1+\sin\varphi'}{1-\sin\varphi'} \quad (3)$$

where φ' is the operative friction angle calculated through an iterative procedure via Bolton's (1986) strength-dilatancy relationships.

Next, A_{ls} is expressed as:

$$A_{ls} = \frac{\pi z}{\cos\psi}\left(z\tan\psi_t + D\right) \quad (4)$$

Therefore, $\frac{dA_{ls}}{dz}$ can be written as:

$$\frac{dA_{ls}}{dz} = \frac{\pi}{\cos\psi_t}\left(2z\tan\psi_t + D\right) \quad (5)$$

Next, using the chain rule:

$$\frac{dN}{dz} = \frac{dN}{dA_{ls}}\cdot\frac{dA_{ls}}{dz} = \frac{pK_p g'_s}{\cos y}\left[\left(d_{crit} + z\right)D + 2z\tan y\, d_{crit} + 2z^2\tan y + \frac{q_o}{g'_s}\left(2z\tan y + D\right)\right] \quad (6)$$

The above equation can be integrated to give the total normal force on the slip plane N as:

$$\int_0^{H_{eff}}\frac{dN}{dz}dz = \left[N\right]_0^{H_{eff}} = \frac{\pi\gamma'_s K_p}{\cos\psi_t}\left[\begin{array}{l}\left(d_{crit} + \frac{1}{2}H_{eff}\right)DH_{eff} + d_{crit}\tan\psi_t H_{eff}^{\ 2} + \frac{2}{3}\tan\psi_t H_{eff}^{\ 3} \\ + \frac{q_o}{\gamma'_s}H_{eff}\left(\tan\psi_t H_{eff} + D\right)\end{array}\right] \quad (7)$$

The last term in the above equation contains the surcharge q_o. The effect of which is to augment the total normal force N and therefore contribute to the sand shearing resistance.

As in Teh (2007) method, the failure plane is a logarithmic spiral with the initial portion of this plane being inclined at an angle ψ_t (see Figure 1 and Figure 2, note that T is the resultant force in Figure 2). The vertical shear force in sand Q_s can be evaluated as,

$$Q_s = \frac{\pi\gamma'_s K_p \sin\left(\varphi_2 - \psi_t\right)}{\cos\varphi_2\cos\psi_t}\left[\begin{array}{l}\left(d_{crit} + \frac{1}{2}H_{eff}\right)DH_{eff} + d_{crit}\tan\psi_t H_{eff}^{\ 2} + \frac{2}{3}\tan\psi_t H_{eff}^{\ 3} \\ + \frac{q_o}{\gamma'_s}H_{eff}\left(\tan\psi_t H_{eff} + D\right)\end{array}\right] \quad (8)$$

where φ_2 is defined as,

$$\varphi_2 = \frac{1}{2}\left(\varphi' + \varphi_{cv}\right) \quad (9)$$

which is mean of the operative and critical state friction angle. If q_o is assumed zero in Equation 8 above, the equation reduces to that of Teh (2007). Also, note that the term ψ_t in this equation is not a dilatancy angle, rather it is a geometric term representing the initial inclination of the logarithmic failure surface and depends on H_s/D and q_{clay}/q_{sand}. Where q_{sand} is the bearing capacity of a foundation resting on sand alone and is given by the following:

$$q_{sand} = \frac{\gamma_s' D}{2} N_{\gamma,cone} + (\gamma_s' d + q_o) N_{q,cone} \quad (10)$$

where, d is the penetration depth corresponding peak with the bearing capacity factors $N_{\gamma,cone}$ and $N_{q,cone}$ defined in Teh (2007).

q_{clay} is the bearing capacity of the clay layer and can be written as:

$$q_{clay} = N_{co} s_{ubi} + q_o \quad (11)$$

Where, N_{co} is taken from Houlsby & Martin (2003) as:

$$N_{co} = 6.34 + 0.56\left(\frac{\rho_{cb} D}{s_{ubi}}\right) \quad (12)$$

Evaluating the clay bearing force at peak, Q_c

Considering the effect of the surcharge, Q_c can be directly evaluated as:

$$Q_c = \pi\left(N_{co} s_{ubi} + H_s \gamma'_s + q_o\right)\left[R^2 - \frac{0.5}{R-r}\left(\frac{2}{3}R^3 + \frac{1}{3}r^3 - R^2 r\right)\right] \quad (13)$$

where R and r are geometric parameters obtained from charts provided in Teh (2007) which are introduced to take into account of the reduction in vertical bearing capacity of clay due to presence of inclined loading (Figure 1). Notice that Q_c reduces to that of Teh (2007) without surcharge.

The weight of the sand frustum (W) is not affected by the surcharge and can be written as:

$$W = \frac{1}{3}\pi H_{eff}\left[\left(\frac{D}{2}\right)^2 + R\frac{D}{2} + R^2\right]\gamma_s' \quad (14)$$

Now q_o can be expressed as products of the top clay height (H_{ct}) and the effective unit weight of top clay (γ_{ct}').

Hence by putting the value of $q_o = H_{ct}\gamma'_{ct}$ to Equations 8 and 13 the final equation for peak bearing force Q from Equation 1 can be rewritten as:

$$Q = \pi\left(N_{co}s_{ubi} + H_s\gamma'_s + H_{ct}\gamma'_{ct}\right)\left[R^2 - \frac{0.5}{R-r}\left(\frac{2}{3}R^3 + \frac{1}{3}r^3 - R^2 r\right)\right] \quad 15$$

$$+\frac{\pi\gamma'_s K_p \sin\left(\varphi_2 - \psi_t\right)}{\cos\varphi_2 \cos\psi_t}\left[\begin{array}{l}\left(d_{crit} + \frac{1}{2}H_{eff}\right)DH_{eff} + d_{crit}\tan\psi_t H_{eff}^{\ 2} + \frac{2}{3}\tan\psi_t H_{eff}^{\ 3} \\ + \frac{H_{ct}\gamma'_{ct}}{\gamma'_s}H_{eff}\left(\tan\psi_t H_{eff} + D\right)\end{array}\right]$$

$$-\frac{1}{3}\pi H_{eff}\left[\left(\frac{D}{2}\right)^2 + R\frac{D}{2} + R^2\right]\gamma_s'$$

If the top clay layer thickness, H_{ct} is set to zero, the above equation reduces to that of Teh (2007) for sand over clay soil without surcharge. This shows the consistency of the newly derived equation which is used to assess the performance of Teh (2007) method against the three layer tests.

Calculating φ_2 in modified Teh method

φ_2 was defined earlier in Equation 9 as the average of the constant volume friction angle (φ_{cv}) and the operative friction angle φ'. In the iterative procedure involving Bolton's (1986) equations suggested by Teh (2007), the mean effective stress p_o' needs to be calculated incorporating the additional vertical stresses from the top clay layer as follows:

$$p_o' = \frac{1}{2}\left[\left(H_{ct}\gamma'_{ct} + \frac{\gamma'_s H_s}{2}\right) + \left(H_{ct}\gamma'_{ct} + \frac{\gamma'_s H_s}{2}\right)K_p\right] = \frac{1}{4}\left[\left(2H_{ct}\gamma'_{ct} + \gamma'_s H_s\right)\left(1 + K_p\right)\right] \quad 16$$

K_p is a function of φ' and was defined in Equation 3. Hence, Equation 16 can be used to arrive at an operative friction angle φ' taking Bolton's (1986) m parameter to be equal to 3. φ' and φ_2 can be evaluated from Equation 9. As φ_{cv} is typically lower than φ', φ_2 is usually smaller than φ'.

REFERENCES

Bolton, M. D. (1986). The strength and dilitancy of sands. *Géotechnique* **36**(1), 65-78.

Houlsby, G. T. & Martin, C. M. (2003.) Undrained bearing capacity factors for conical footings on clay. *Géotechnique* **53(5)**:513-520.

Teh, K. L. (2007). *Punch-through of spudcan foundation on sand overlying clay.* PhD thesis, National University of Singapore.

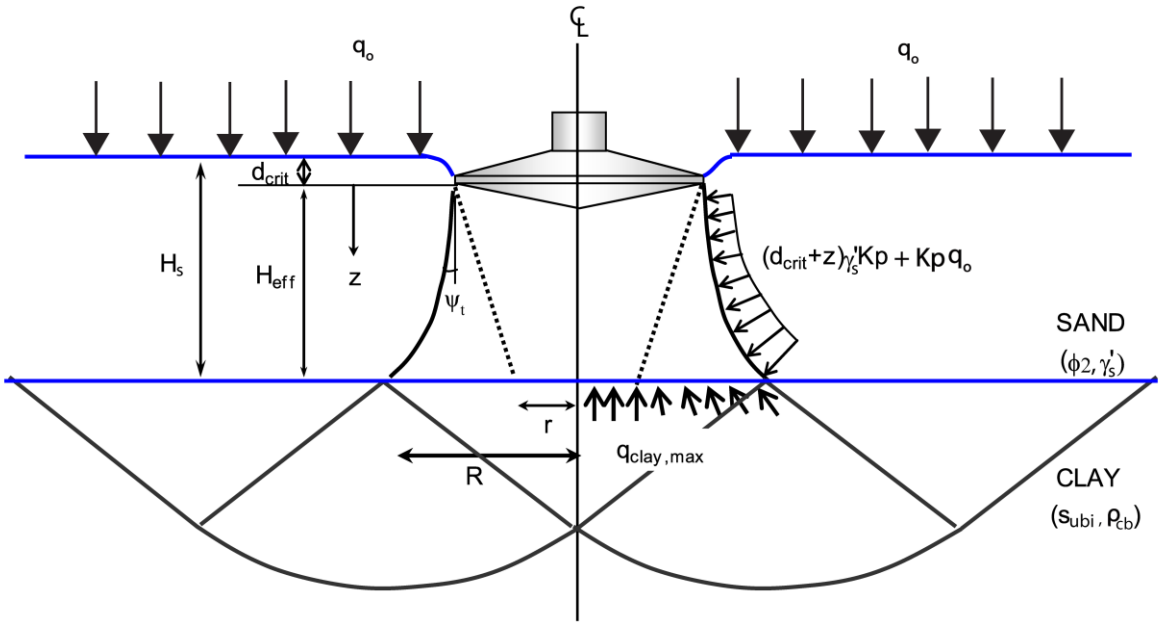

Figure 1: Extended Teh (2007) model with added surcharge q_o (modified after Teh, 2007)

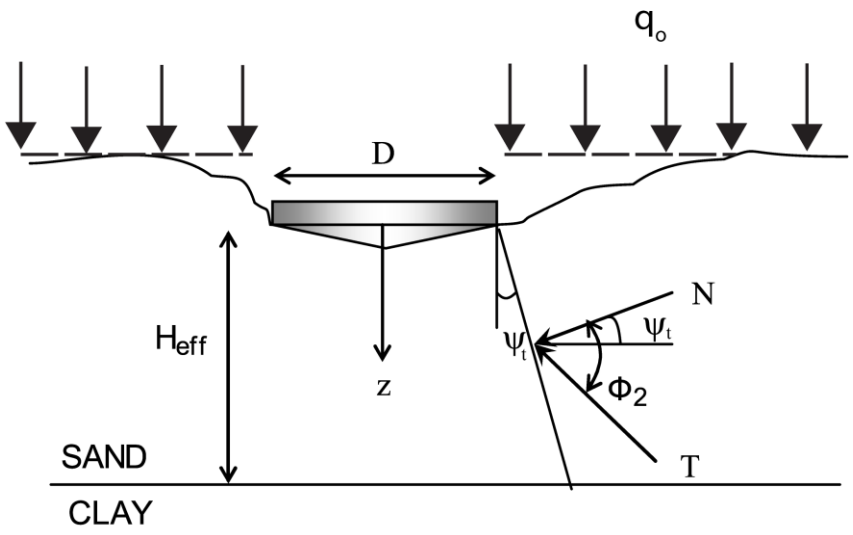

Figure 2: Simplified force diagram on sand failure surface, N is the total normal force and T is the resultant force (modified after Teh, 2007)

Journal: **Geotechnique**
Article number: **16-P-101R1**
Title: **Foundation punch-through in clay with sand: analytical modelling**
Author(s): **Shah Neyamat Ullah, PhD; Samuel Stanier, PhD; Yuxia Hu; David White**
Article type: **General Paper**

Note: All changes made to the manuscript in this revision have been highlighted in purple in the revised manuscript.

Reviewer #1: General comments The paper is clearly written and addresses and important issue with regards the safety of offshore jack up rigs and punch-through predictions. The work includes the development of an analytical design methodology that is a step forward in layered soil design and would make an important contribution to practice. The reviewer requires re-assurance that the elevated bearing pressures are not as a result of modelling issues. See companion paper comments. Additional comments here are generally of a typographical nature only.	We thank the reviewer for taking the time to re-review our paper. We have carefully addressed the remaining concerns regarding modelling issues in the revised version and have provided additional explanations with regards to boundary effects in reply to the companion paper (see comment 1).
Detailed comments 1. Introduction Page 3, para 2, line 17 & 24, are brackets missing from reference date?	Missing brackets have been added.
2. Extended stress dependent… Page 4, line 46, as mentioned in companion paper "over- and underlying clay" may be better as "over, and underlying clay"?	We agree and have adjusted this throughout both papers.
3. Mathematical formulation for peak resistance Page 9, para 2, line 39, suggest replace "relation" with "relationship".	Replaced as suggested.
4. Prediction method for… Page 13, para 1, line 44, as mentioned in companion paper "over- and underlying clay" may be better as "over, and underlying clay"?	Adjusted as suggested.

5. Page 14, para 1, lines 8-10, check "is" or "are" adopted, may need to change "factor" to "factors".	Changed ‘are’ to ‘is’ reflecting singular factor.
6. Performance of full resistance…. Page 19, bullet point 1, line 36, Reference to coloured markers, see comments in companion paper.	This has been answered in reply to the companion paper review (please see comment 8).
7. Conclusions Page 23, Bullet point 6, line 27-28, remove the text "are universal as they" as this is misleading and implies that the approach can be used in all cases (may be misinterpreted by a reader) and goes against the reviewer's previous request to caveat findings.	Removed as suggested.
8. References As per comments in companion some conference papers are missing page numbers and full referencing. Update where possible.	The references have been checked and updated. Missing page numbers on conference papers have been added including OTC paper numbers.

Reviewer #2: The Reviewers Comments have been appropriately addressed and incorporated in the revised version of the Manuscript. The quality of the figures has been substantially improved. The revised Manuscript is well-written, the numerical approach is nicely presented and the conclusions are adequately justified.	We thank the reviewer for taking the time to re-review our paper.

Journal Publishing Agreement

It is our policy to ask authors to assign the copyright of articles accepted for publication to the Publisher. Exceptions are possible for reasons of national rules or funding. Please tick the relevant options below.

In assigning copyright to us, you retain all proprietary rights including patent rights, and the right to make personal (non-commercial) use of the article, subject to acknowledgement of the journal as the original source of publication.

By signing this agreement, you are confirming that you have obtained permission from any co-authors and advised them of this copyright transfer. Kindly note that copyright transfer is not applicable to authors who are opting to publish their papers as Open Access. Open Access authors retain copyright of their published paper.

Please complete the form below and return an electronic copy to your ICE Publishing contact: (http://www.icevirtuallibrary.com/info/submit).

Journal name: Géotechnique

Article title: Foundation punch-through in clay with sand: analytical modelling

Manuscript reference number: 16-P-101R2

Authors: Shah Neyamat Ullah, Samuel Stanier, Yunia Hu, David White

Your name: Shah Neyamat Ullah

Signature and date: 21/11/2016

Please tick either one option from part A or one option from part B. Please complete part C.

A. Copyright

- [x] I hereby assign and transfer the copyright of this paper to Thomas Telford Ltd.
- [ ] British Crown Copyright: I hereby assign a non-exclusive licence to publish to Thomas Telford Ltd.
- [ ] I am a US Government employee: employed by (name of agency) .....
- [ ] I am subject to the national rules of (country) ..... and confirm that I meet their requirements for copyright transfer or reproduction (please delete as appropriate)

B. Authors with open access funding requirements. Please specify the Creative Commons license version required.

- [ ] CC-BY (for full details click here Creative Commons Attribution (CC BY) 4.0 International License)
- [ ] CC-BY-NC-ND (for full details click here Creative Commons Attribution Non Commercial No-derivatives (CC BY NC ND) 4.0 International License)

C. Please confirm that you have obtained permission from the original copyright holder. For ICE Publishing's copyright policy, please click here. ICE Publishing is a signatory to the STM Guidelines.

- [ ] I have obtained permission from the original copyright holder for the use of all subsidiary material included in this paper (E.g. for borrowed figures or tables).

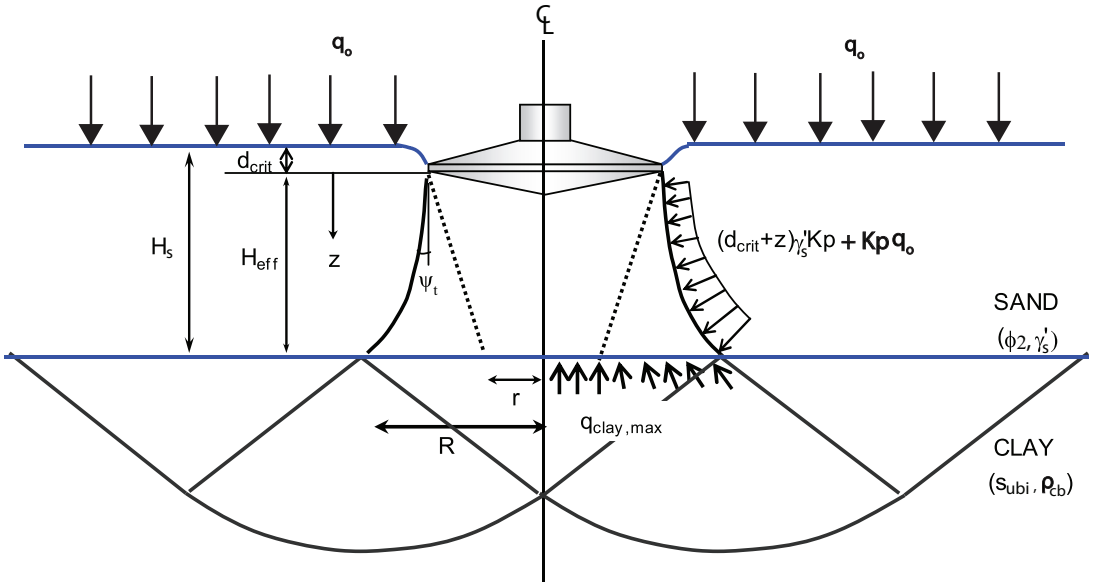

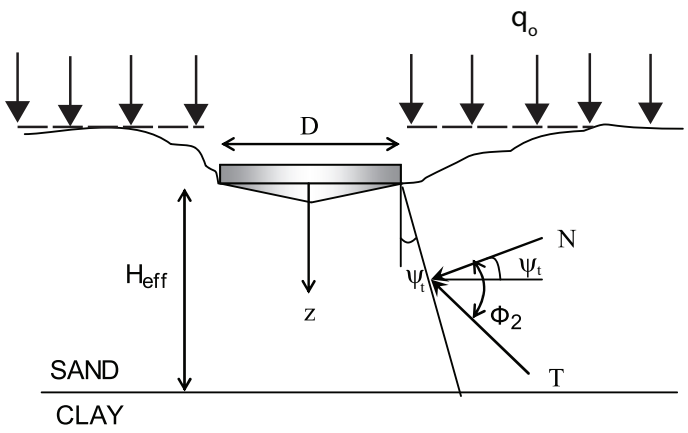

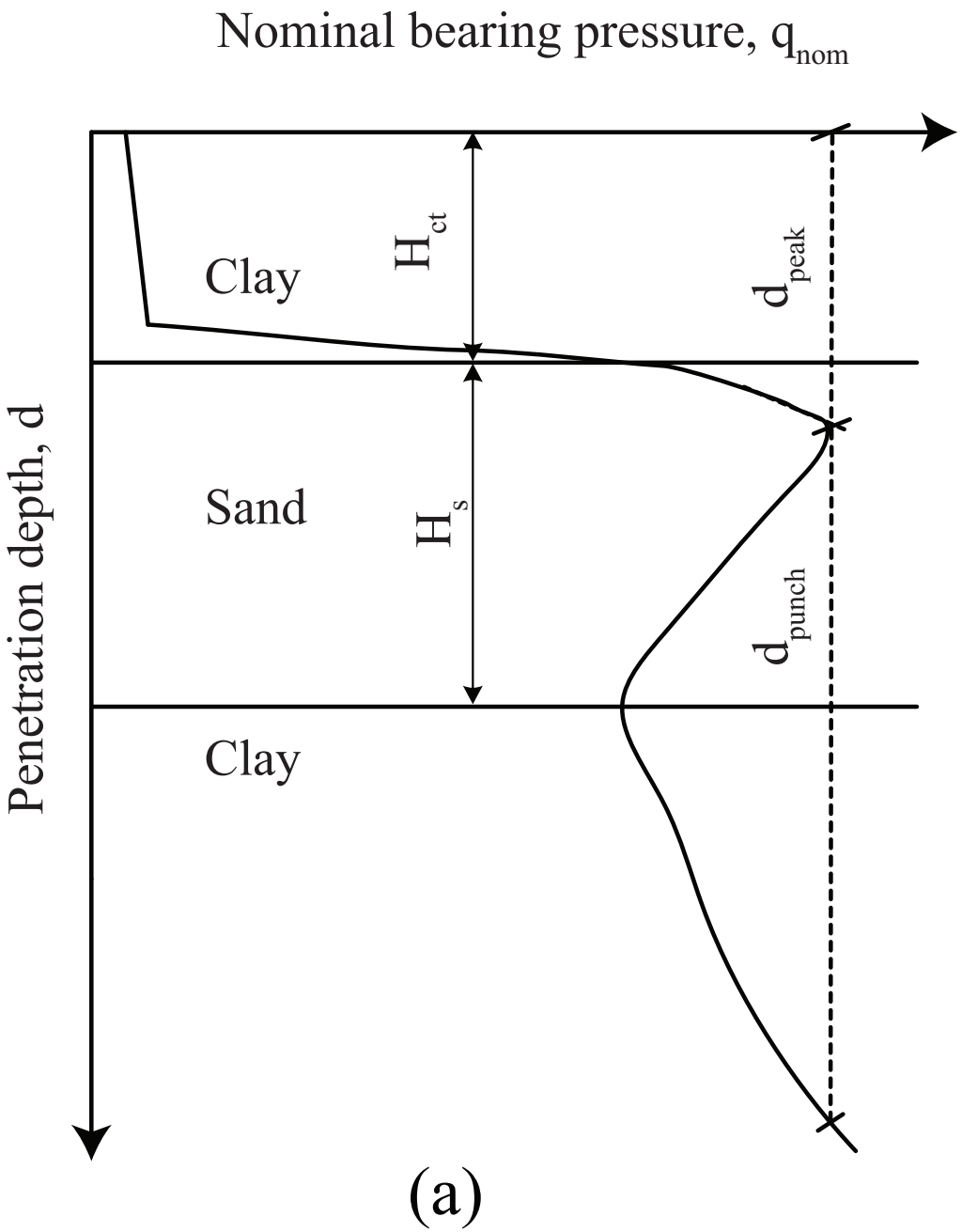

(a)

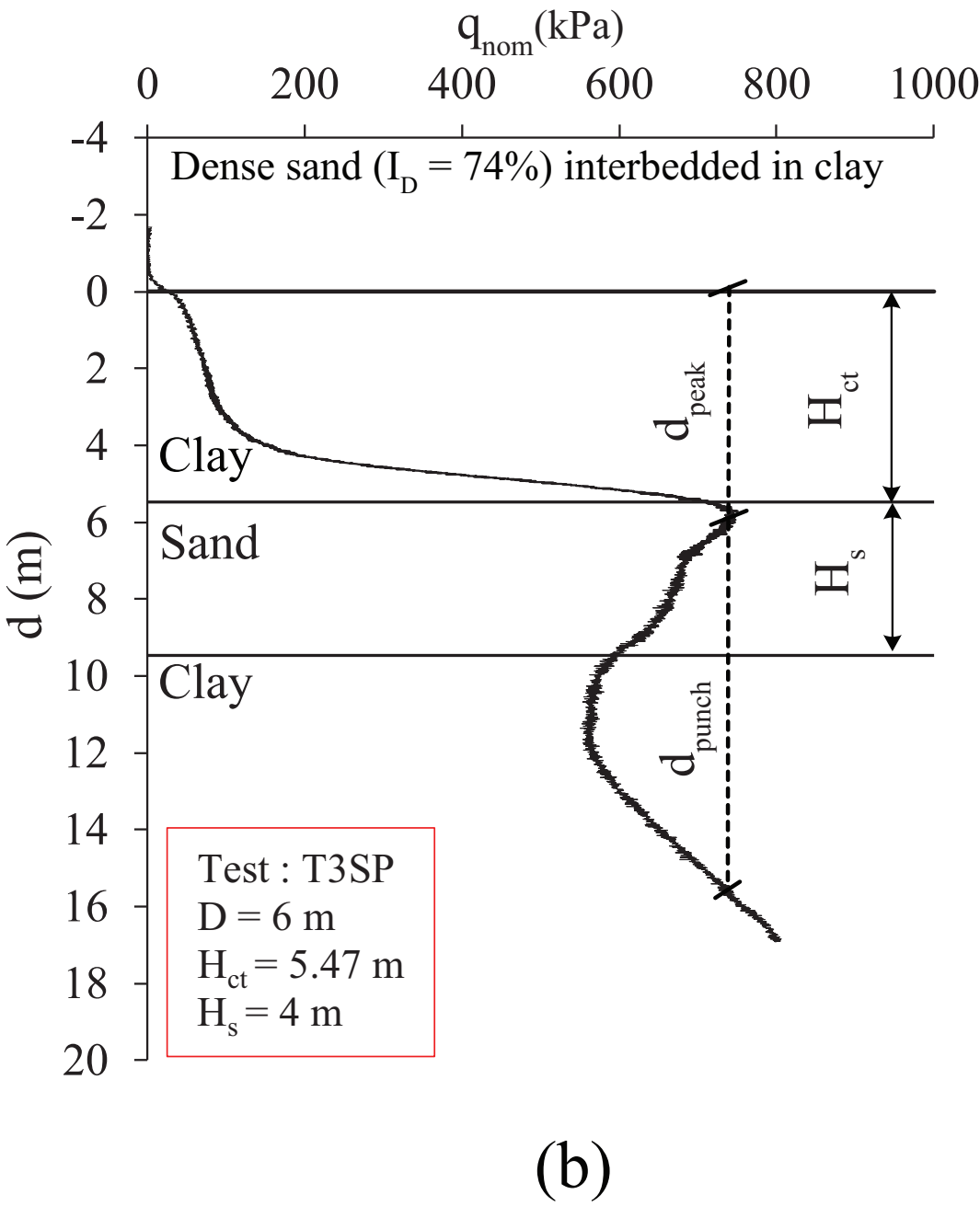

(b)

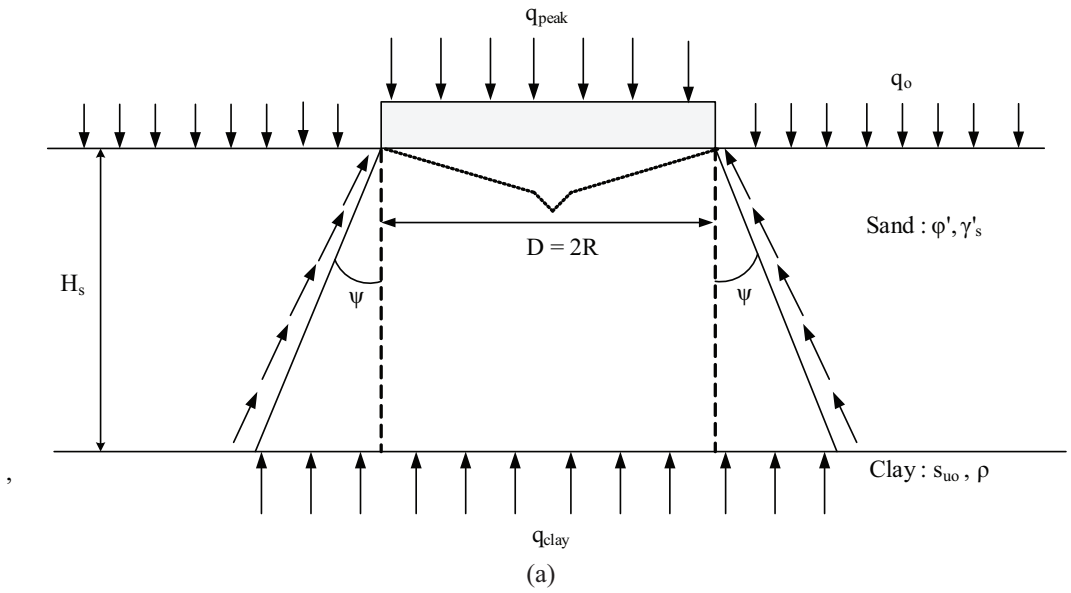

(a)

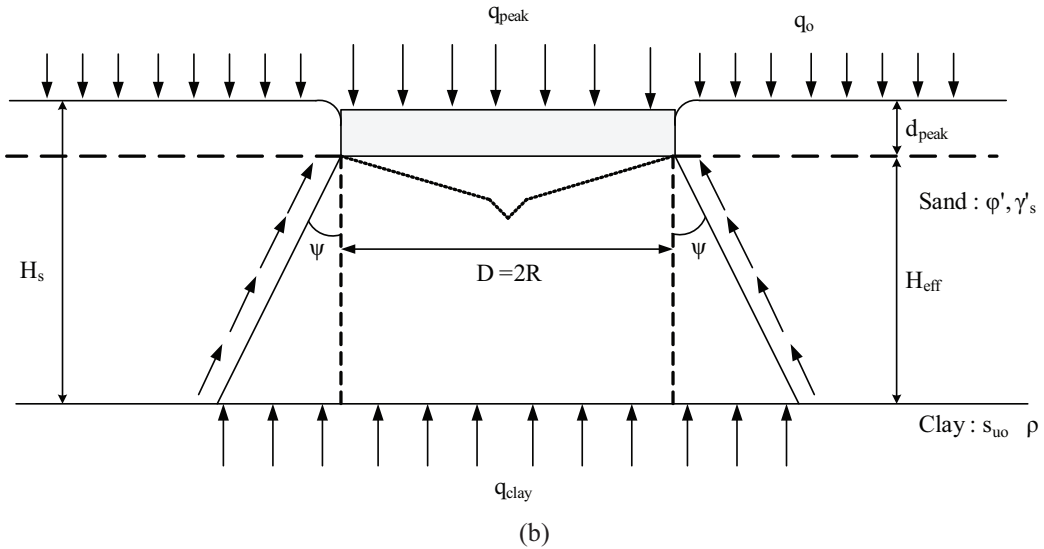

(b)

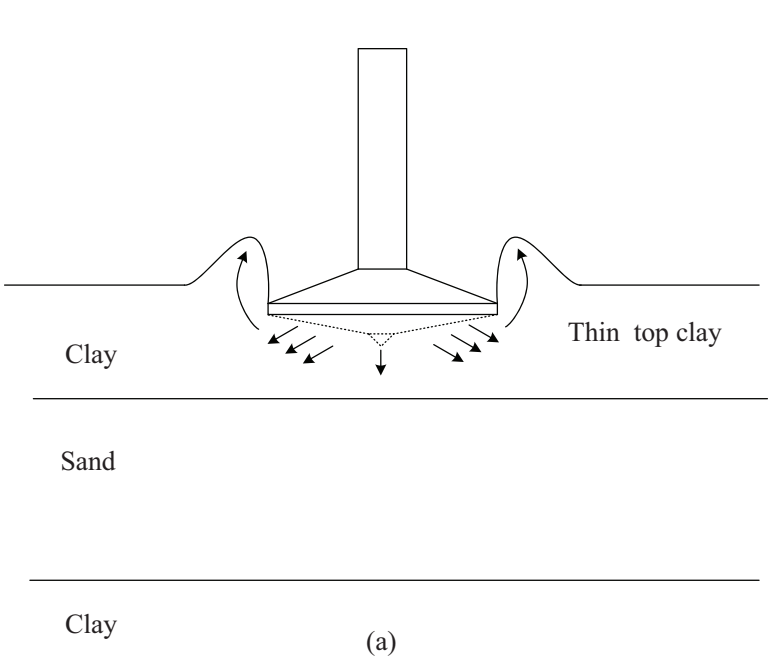

(a)

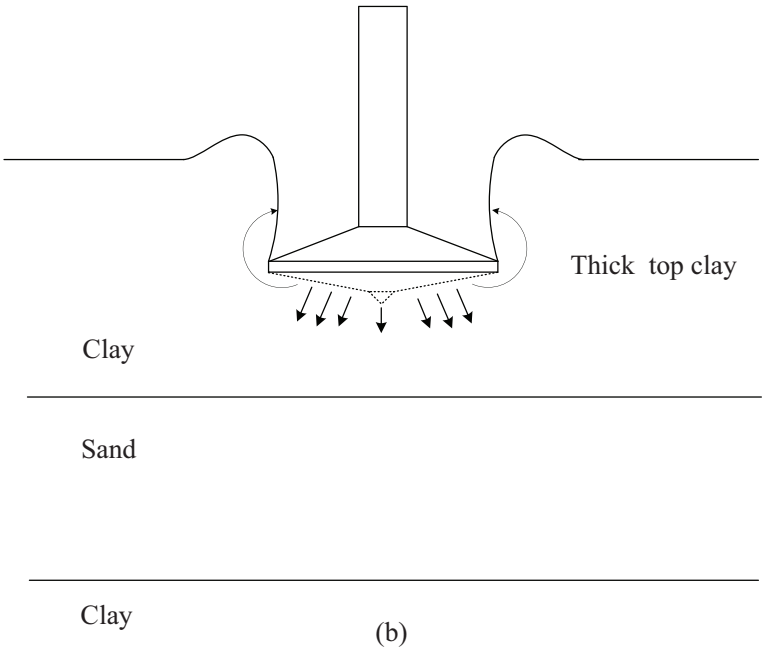

(b)

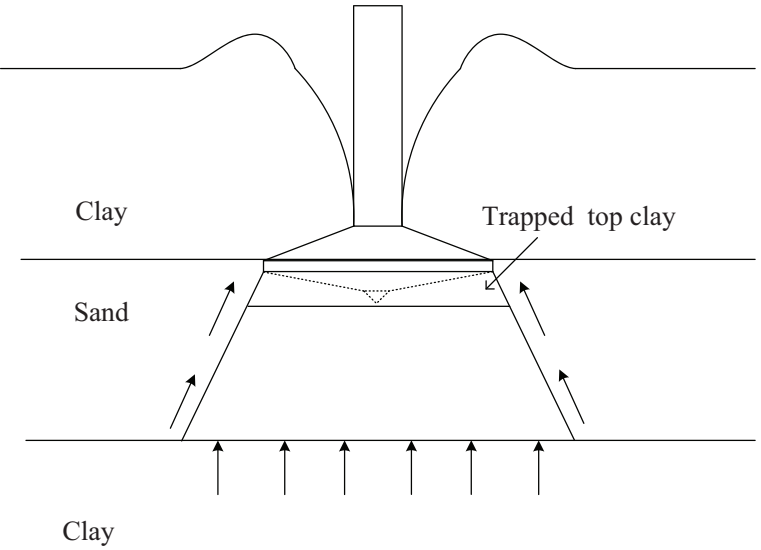

(c)

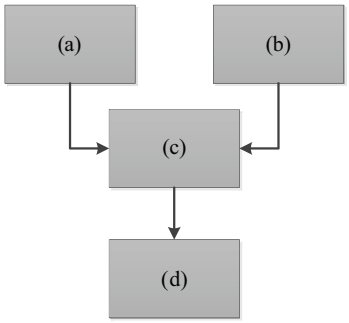

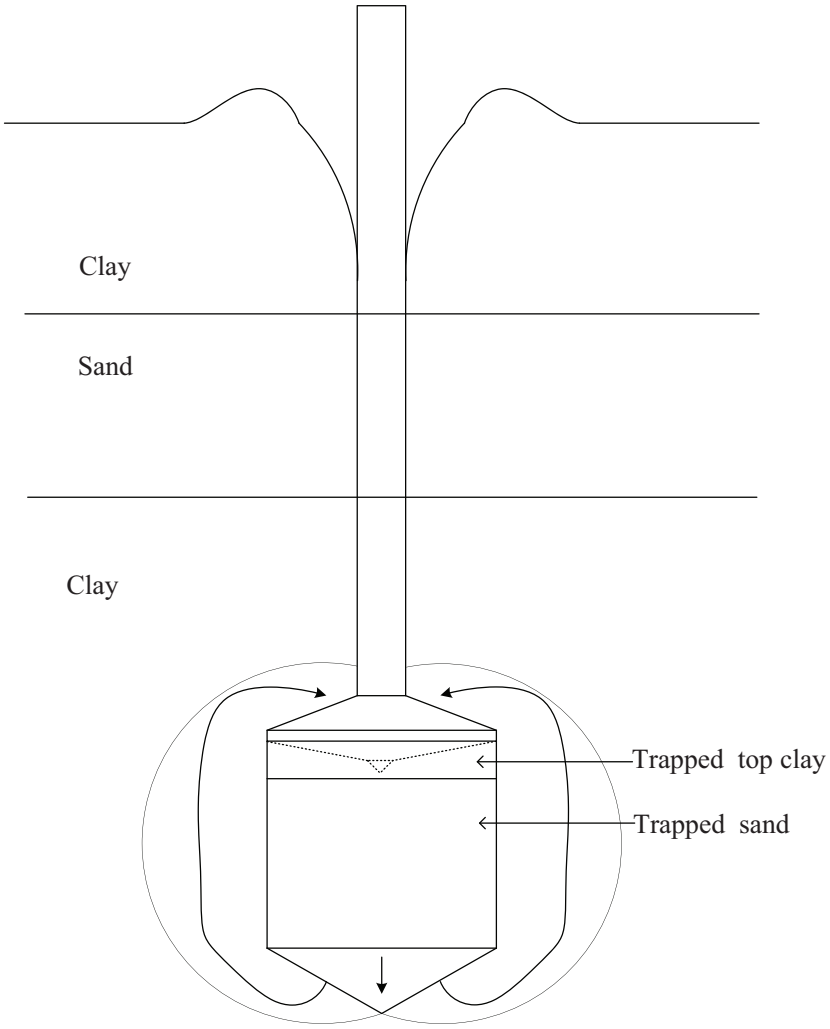

(d)

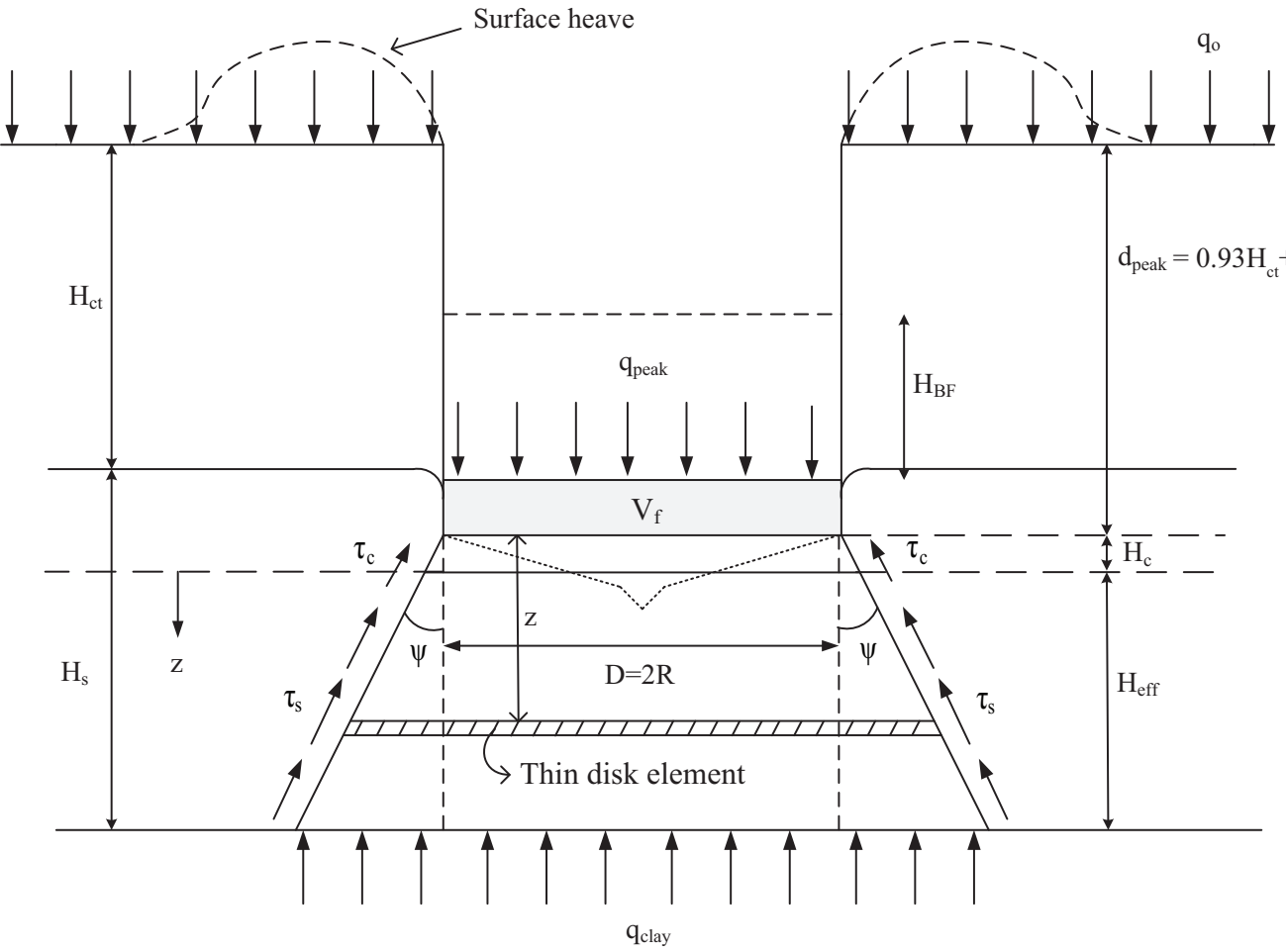

(a)

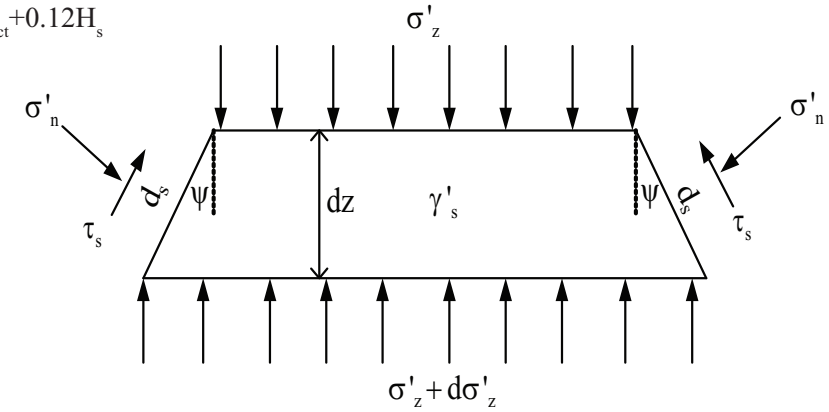

(b)

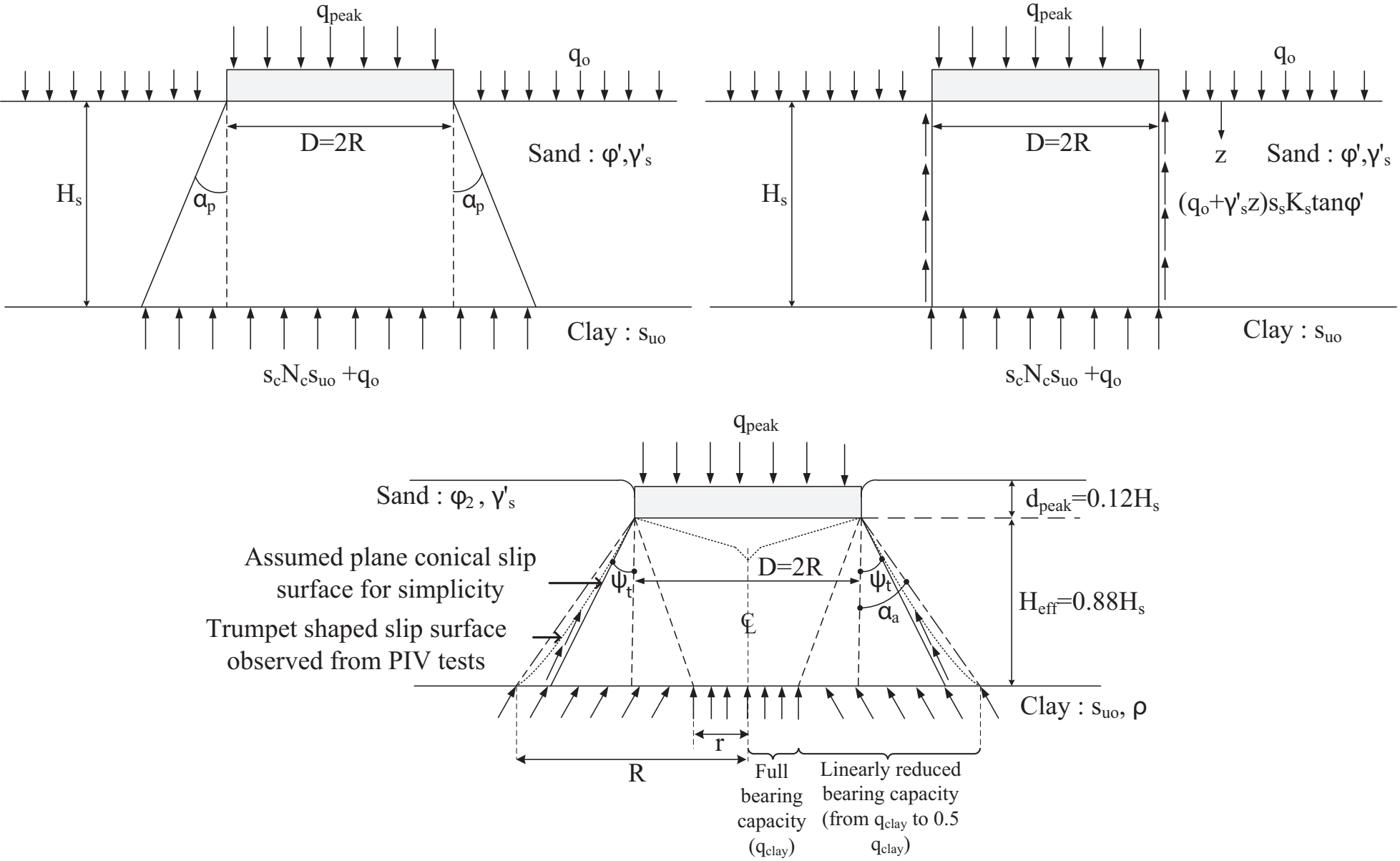

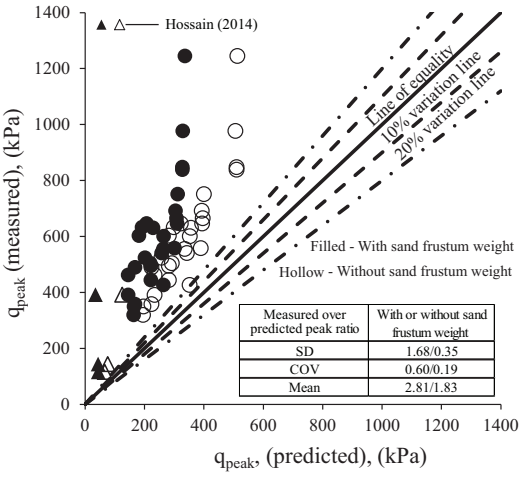

(a) SNAME/ISO projected area (1h:3v)

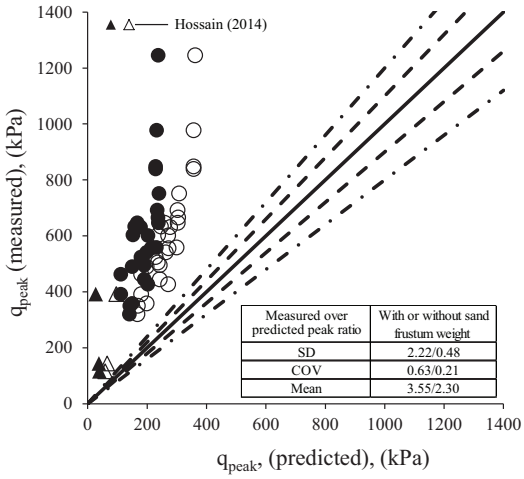

(b) SNAME/ISO projected area (1h:5v)

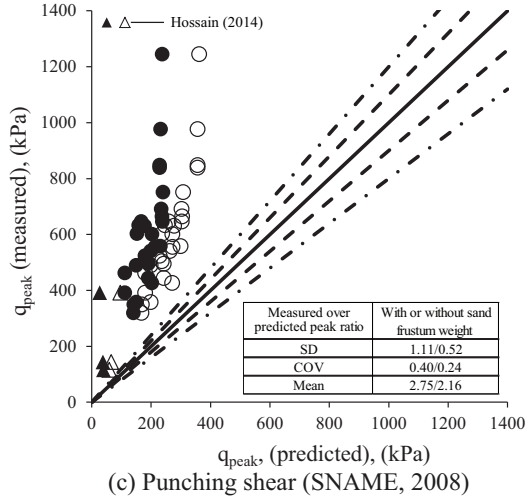

(c) Punching shear (SNAME, 2008)

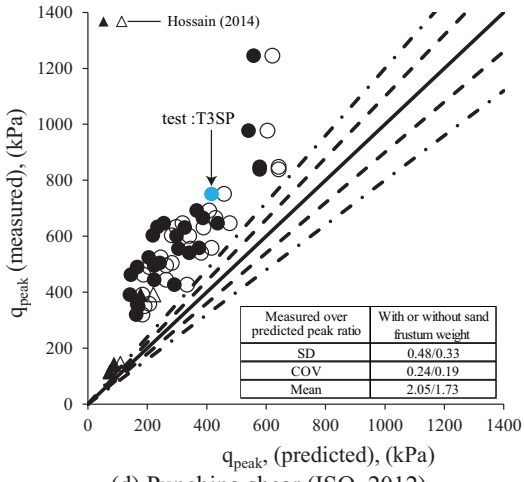

(d) Punching shear (ISO, 2012)

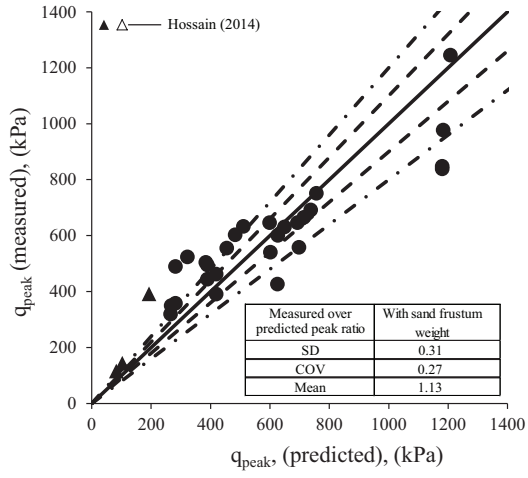

(e) Teh's approach (extended) (2007)

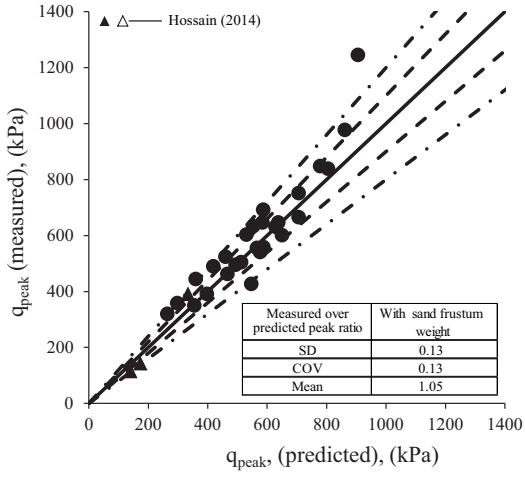

(f) Proposed approach

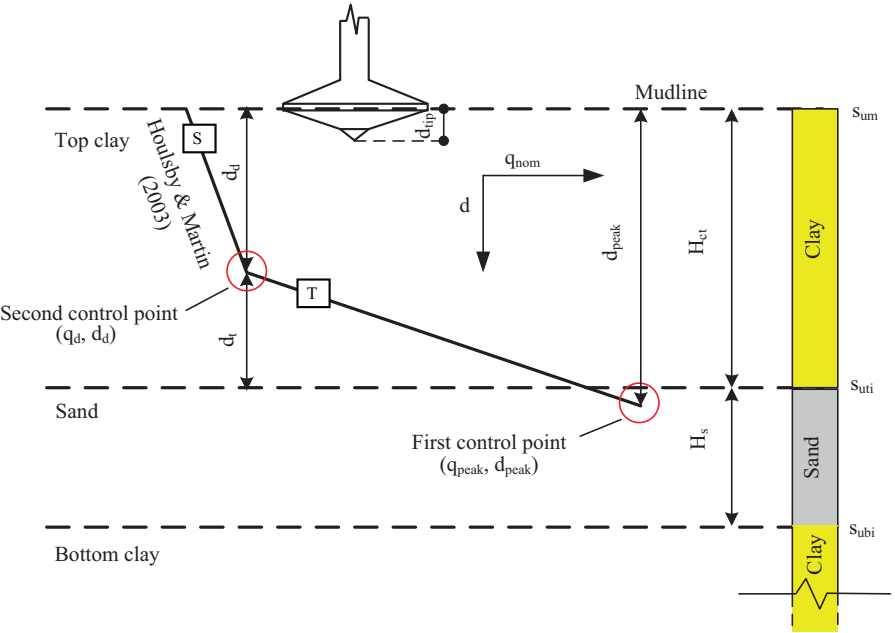

(a)

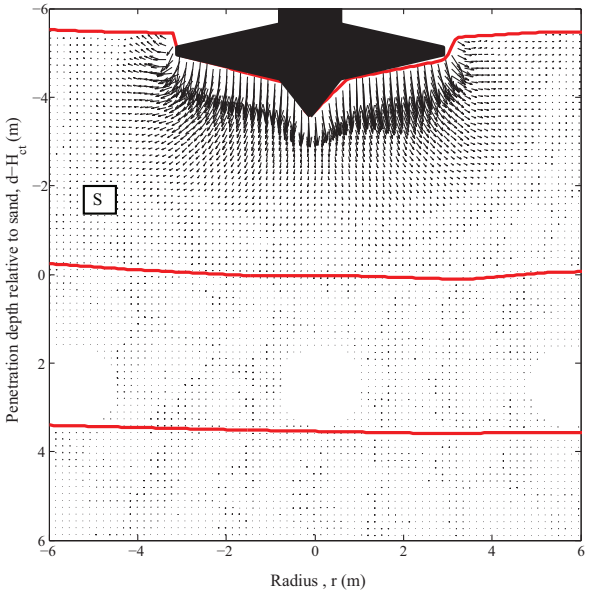

(b)

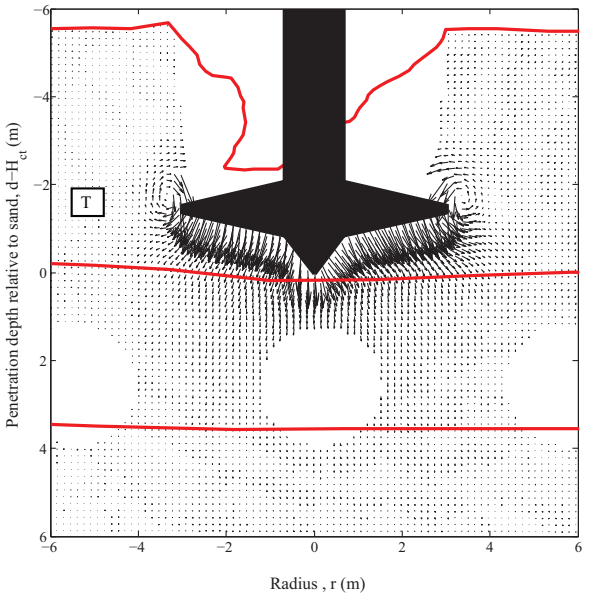

(c)

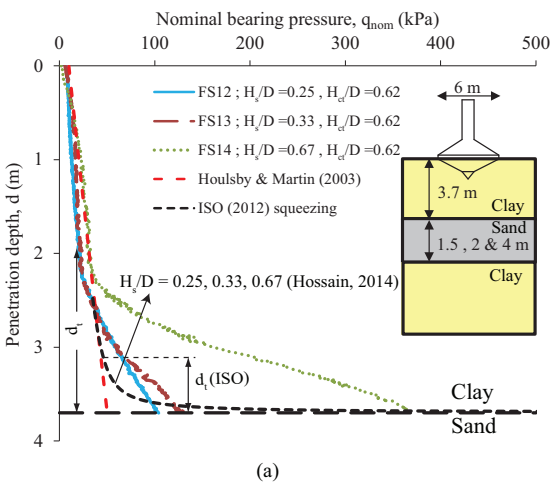

(a)

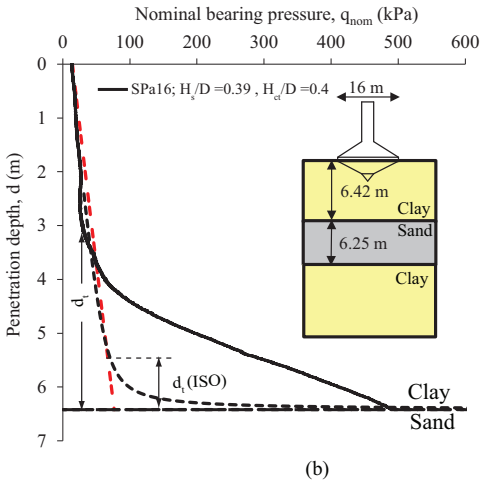

(b)

Click here to download Figure Figure 9.eps

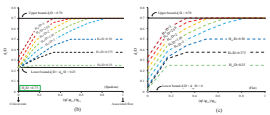

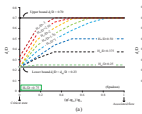

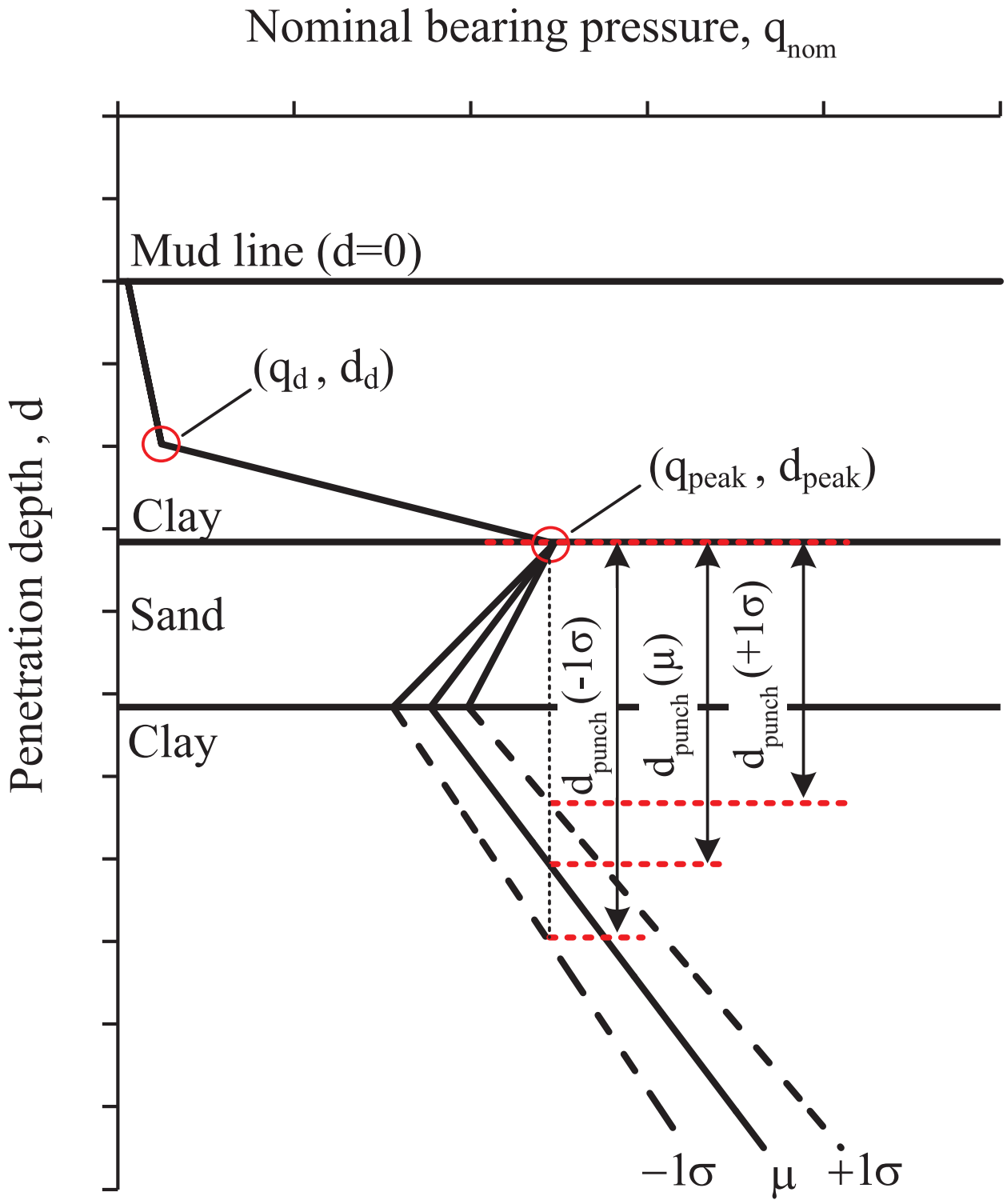

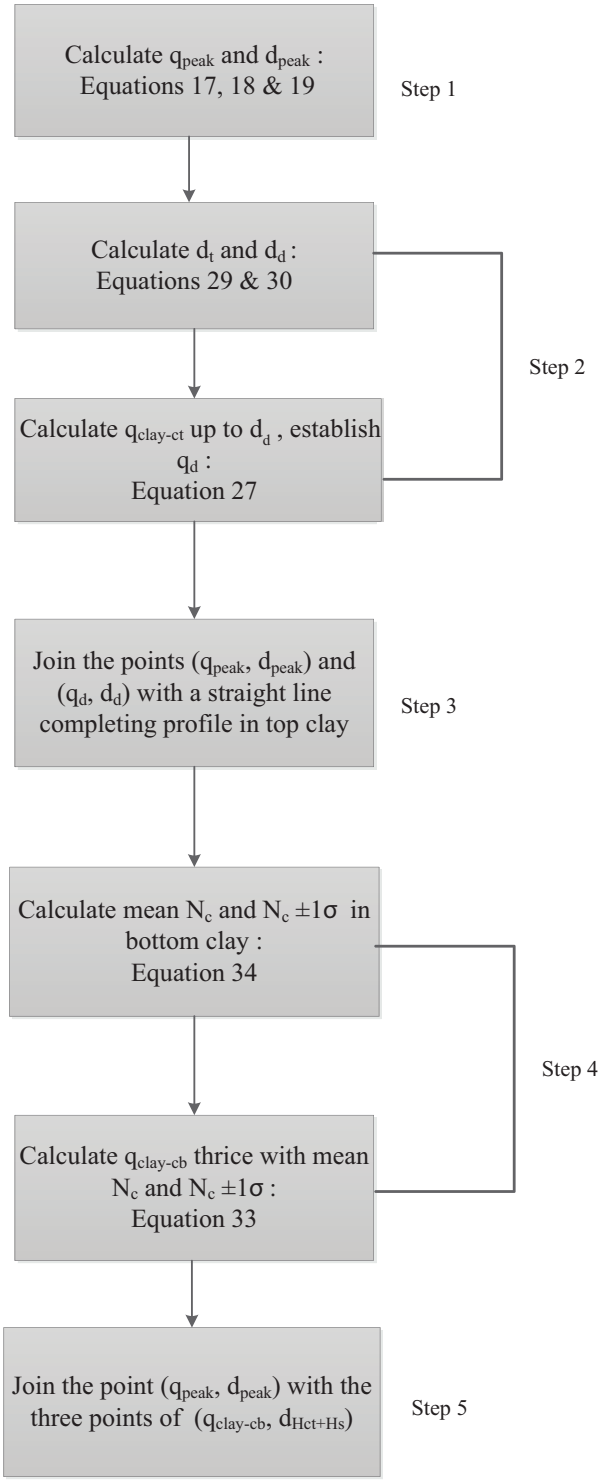

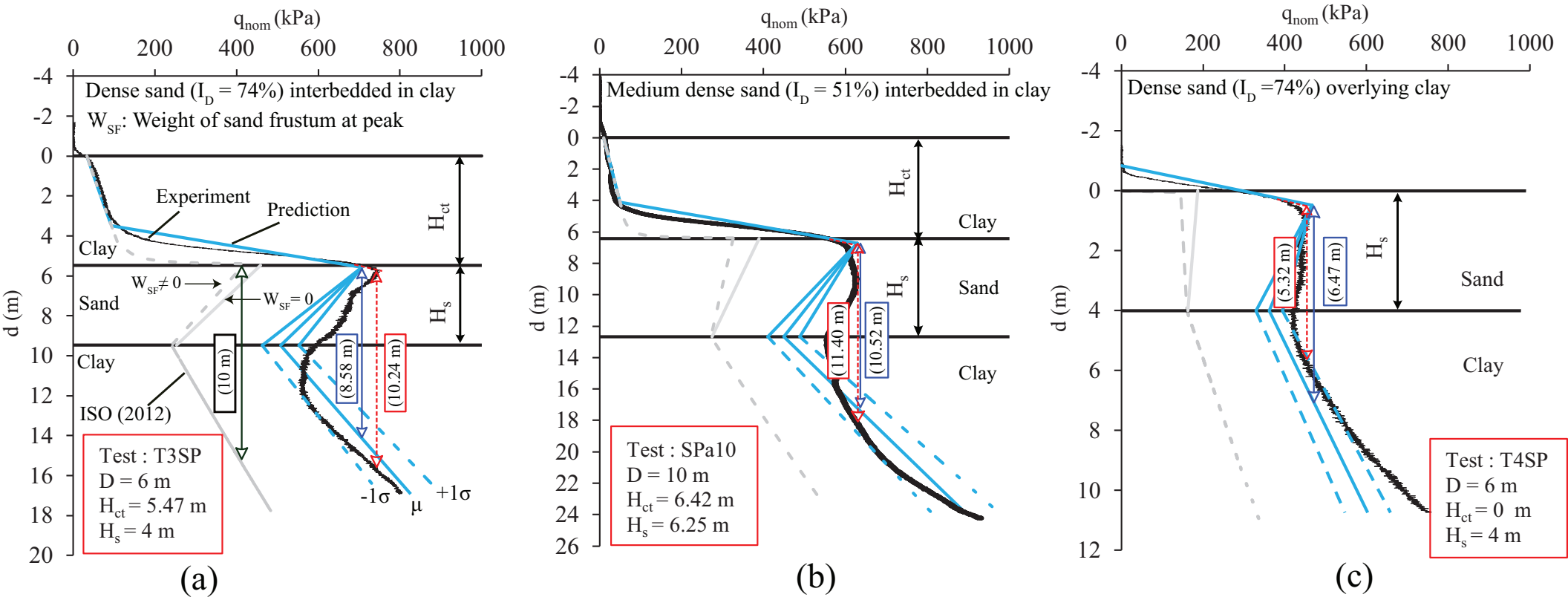

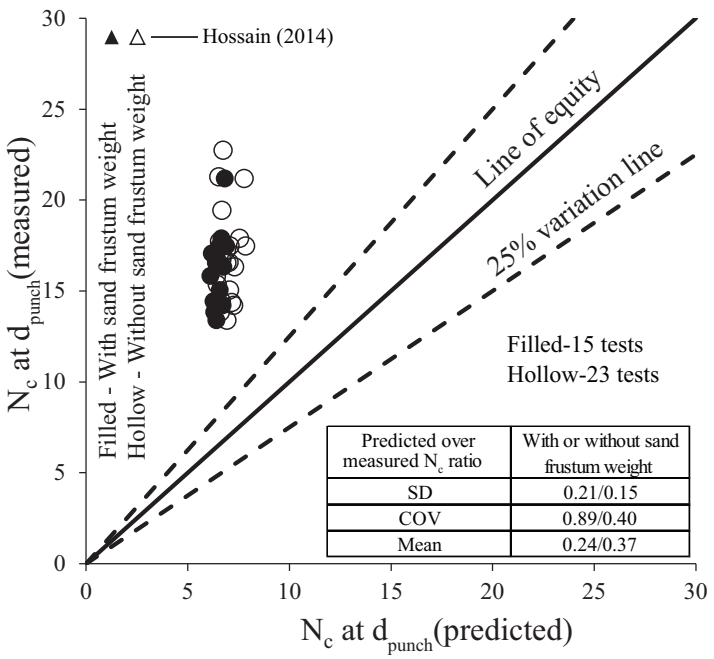

(a) SNAME/ISO projected area (1h:3v)

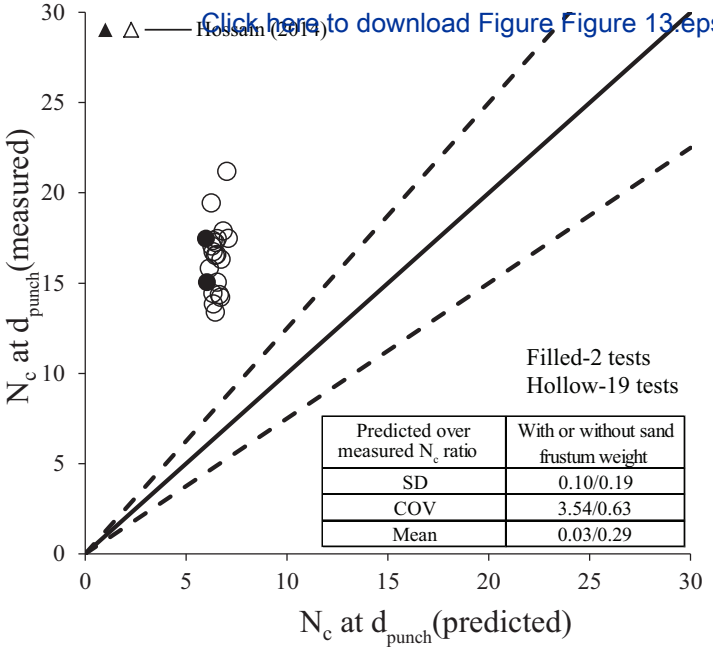

(b) SNAME/ISO projected area (1h:5v)

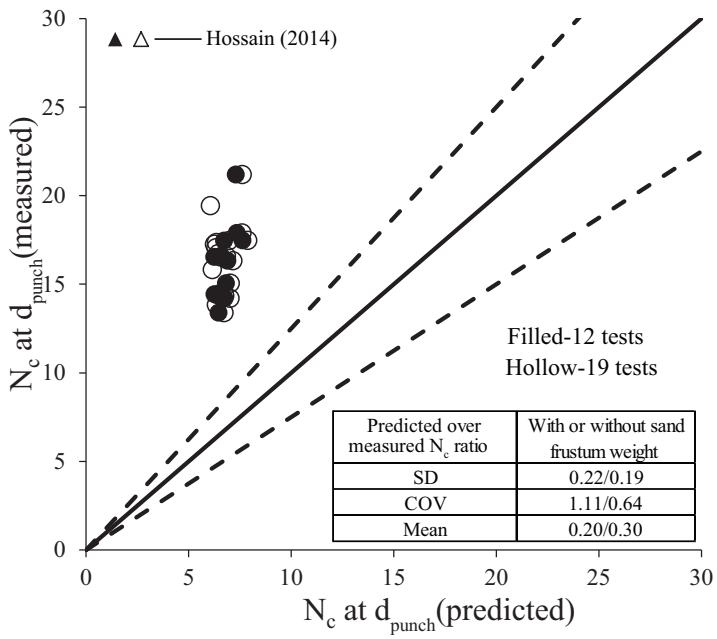

(c) Punching shear (SNAME, 2008)

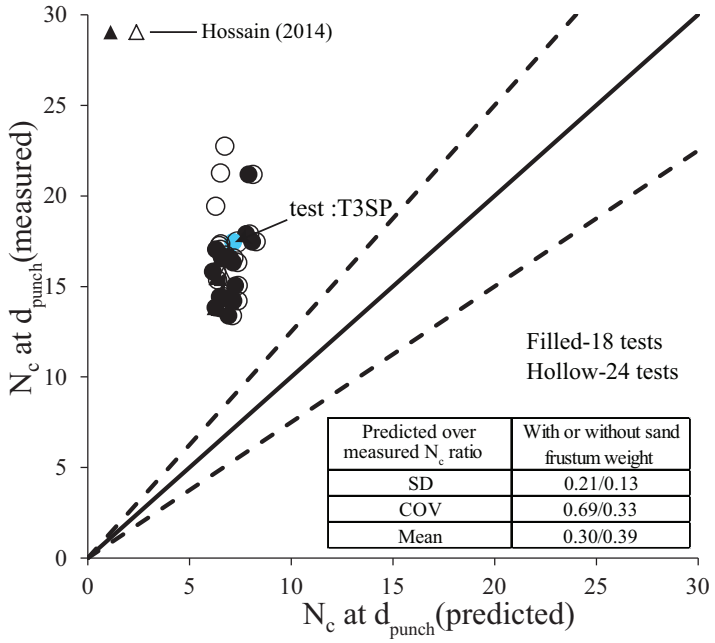

(d) Punching shear (ISO, 2012)

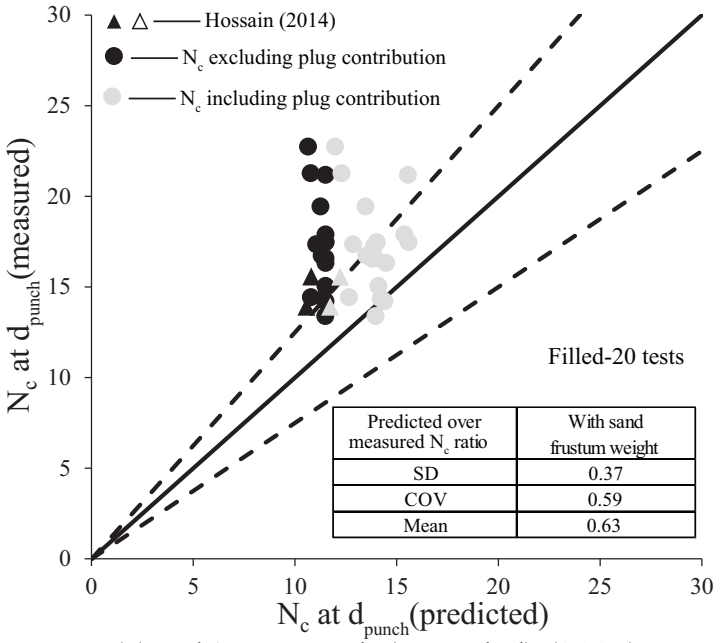

(e) Teh's approach (extended) (2007)

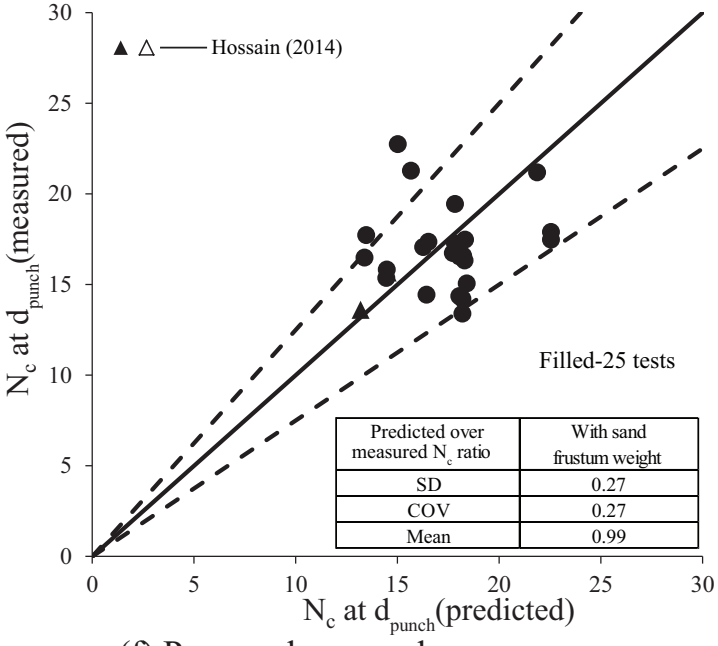

(f) Proposed approach

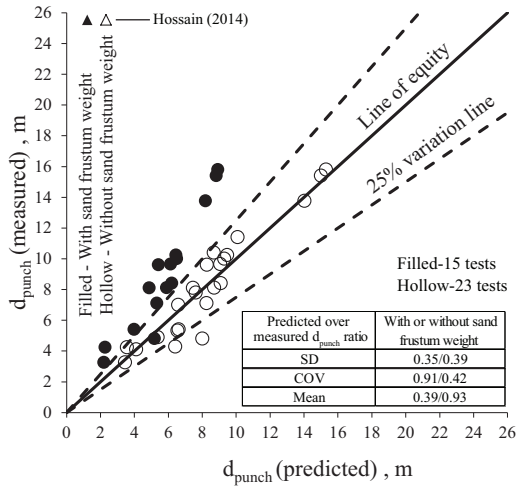

(a) SNAME/ISO projected area (1h:3v)

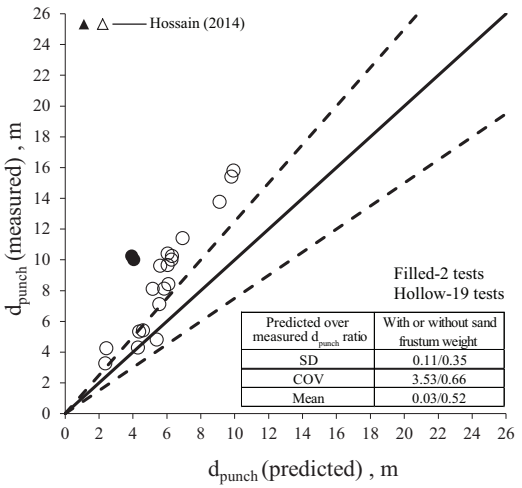

(b) SNAME/ISO projected area (1h:5v)

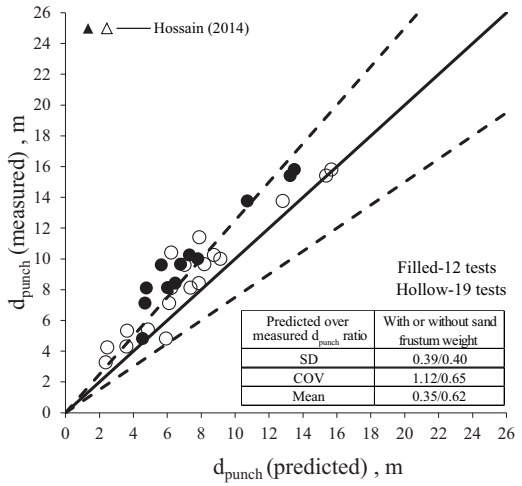

(c) Punching shear (SNAME, 2008)

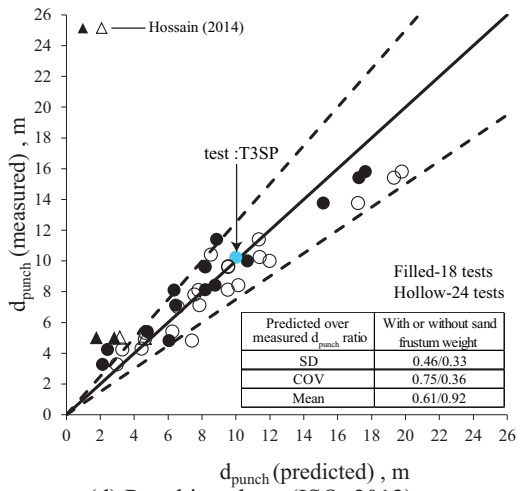

(d) Punching shear (ISO, 2012)

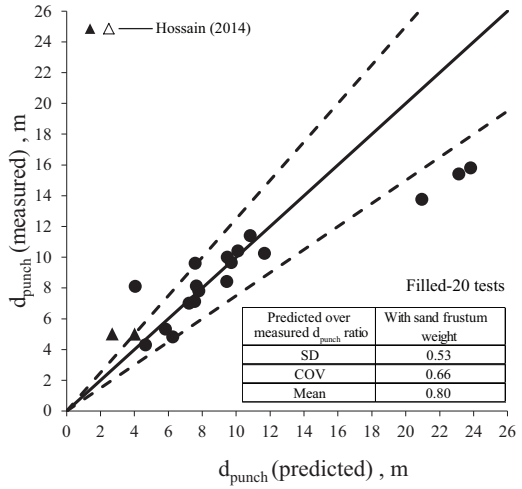

(e) Teh's approach (extended) (2007)

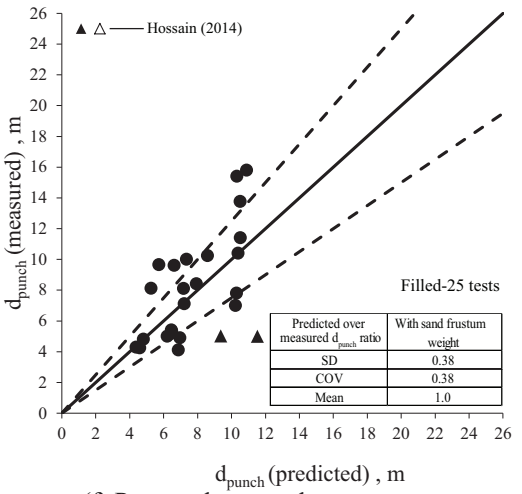

(f) Proposed approach

Table 1: Parameters required for predicting peak resistance q_{peak}.

Parameter category	Symbol	Description	Method of determining parameter
Foundation geometry	D & V_f	Foundation diameter and volume	Known parameters
Top clay	H_{ct}	Top clay height	Measured in situ
	H_c	Height of trapped clay	Taken as $f_1 H_{ct}$ with $f_1 = 0.07$.
	s_{um}	Mud line undrained shear strength	Measured in situ or in laboratory tests.
	ρ_{ct}	Top clay strength gradient	Measured in situ.
	γ'_{ct}	Top clay unit weight	Inferred from in situ tests or directly measured in the laboratory.
	f_1	Factor determining the amount of top clay entrappment	Taken as 0.07. Suggesting on average 7% of the top clay gets entrapped under the foundation.
	f_2	Factor determining the height of backfill	f_2 is taken as 0.50 (half backfill condition).
Sand	H_s	Sand height	Measured in situ.
	I_D	Sand relative density	Measured in the laboratory from undisturbed samples or in situ.
	Q	Parameter in Bolton (1986) equation	Measured from laboratory tests, For siliceous sand can be taken as 10.
	I_R	Relative density index	Obtained through an iterative procedure involving Equations 17, 23, 24 & 25.
	φ_{cv}	Constant volume friction angle	Measured from laboratory tests.
	φ' & ψ	Operative friction and dilation angle	Obtained from Equations 24 & 25 : $\varphi' = \varphi_{cv} + 2.65 I_R$ & $0.8\psi = \varphi' - \varphi_{cv}$, $\psi \geq 0$
	φ^*	Reduced friction angle due to non-associated flow of sand	Obtained from Equation 3 : $\tan\varphi^* = \frac{\sin\varphi'\cos\psi}{1-\sin\varphi'\sin\psi}$
	γ'_s	Effective unit weight of sand	Inferred from in situ tests or directly measured in the laboratory.
Bottom clay	s_{ubi}	Bottom sand-clay intercept strength	Measured in situ.
	ρ_{cb}	Bottom clay strength gradient	Measured in situ.
	κ	Non dimensional strength parameter needed to determine the bearing capacity factor from (Houlsby and Martin, 2003).	Calculated from Equation 11: $\kappa = \frac{\rho_{cb}\left\{D + 2\left(H_{eff} + H_c\right)\tan\psi\right\}}{s_{ubi}}$; H_{eff} is taken as $0.88H_s$.
	N_{co}	Bottom clay bearing capacity factor	Calculated from Equation 10: $N_{co} = 6.34 + 0.56\kappa$ (Houlsby and Martin, 2003)
Empirical factor	D_F	Distribution factor: Defined as the ratio of the normal effective stress at the slip surface to the mean vertical effective stress within the sand frustum.	For spudcan use Equation 6: $D_F(\text{spudcan}) = 0.642\left(\frac{H_s}{D}\right)^{-0.576}$; $0.16 \leq \frac{H_s}{D} \leq 1.0$ For flat foundation use Equation 7: $D_F(\text{flat}) = 0.623\left(\frac{H_s}{D}\right)^{-0.174}$; $0.21 < \frac{H_s}{D} < 1.12$